A Combination of Enhanced Watershed Algorithm with SVM phenomena for Liver Cancer

Name of Research Scholar

Name: ABC

Roll No:

Class: M.Phil.

Session: 2018-2020 Fall

Introduction to Supervisor

Name: Dr.

Designation: Associated Dean

Department: Computer Science

Institution: Minhaj University

School of Computer Science

Faculty of Computer Science & Information Technology

MINHAJ UNIVERSITY LAHORE HAMDARD

CHOWK TOWNSHIP LAHORE

Abstract

In this research I study that apply enhanced watershed algorithm with SVM phenomena as an active detection tool for liver cancer, remove undetected lesions of liver cancer by using enhanced watershed algorithm and SVM phenomena, evaluate the efficiency of EWA (Enhanced Watershed Algorithm) with SVM against prior algorithm for liver cancer detection and check the level of undetected possibility of liver cancer with the present algorithms and EWA with SVM phenomena. By reviewing different factors related to the research it is derived that the research methodologies is based on enhanced, correlated, modified and particularly focused on various aspects and factors of research paradigm. The theoretical knowledge of the research reflects that our research is based on secondary research by unrevealing different features and gets the desired objectives by emphasizing on previous theoretical concepts. By jumping towards the practically implementations of the research the theoretical methodologies are molded in such a way where quantitative and analyzing images of patient's datasets are in used and collected from different hospitals which is based on liver cancer prediction and detection purpose. Sudhamani et al. (2014) also adopted the similar approach to test 100 CT images of 63 patients by using MATLAB. Hence by using enhanced algorithm better accuracy is obtained and through images datasets detection and prediction phenomena is succeeded. It happens to be only reliable approach that achieves efficient accuracy and better prediction and detection results. In this work, the tumour region is detected and segmented in the liver CT picture. A vector support machine is used to diagnose the segmented liver tumour, which subsequently classifies the liver tumour as benign or malignant. Sensitivity, specificities, optimistic prognostic value, adverse predictive value and accuracy are then analysed.

Keyword: Liver Tumour, CT scan, SVM

Chapter: 01

Introduction

1.1 Background of study

Disease is the second important cause of impermanence universal. According to WHO data, it was liable for 8.8 million fatalities in 2015, with 788,000 of those fatalities owing to liver cancer (WHO, 2020). According to the American Cancer Society, there will be around 42,810 confirmed cases (30,170 males and 12,640 women) diagnosed in 2020, with 30,160 people (20,020 men and 10,140 women) dying from primary liver cancer and based on inter biliary cancer in the U.s alone (ACS, 2020).

The liver is the major gland in the physique and a crucial metabolic function. The liver is responsible for digesting, filtration, and metabolic. Based on the aetiology of the illness, active and passive liver cancers are separated into two types. Main liver tumor is a tumor that instigates in the cells of the liver. Hemangioma Liver cirrhosis and hepatorenal syndrome are two types of primary liver cancer. Hepatocellular carcinoma (HCC) is the most predominant symbol of liver cancer, which arises when cancer cubicles originate in the liver's cells. A hemangioma is a plasma vessel network in the liver (Bosch et al., 2004). Secondary metastatic liver cancer occurs when tumor extents from alternative segment of the body. (Ananthakrishnan et al., 2006).

A liver disease improves the shape and texture of the liver. The liver, its veins, and tumours must all be removed and correctly portioned in order to detect the condition. Unfortunately, due to the seriousness of homogeneity inside the liver, the low contrast's form and the existence of neighbouring large intestines, effective liver separation is challenging. To detect liver disordersUltrasonic, for example, is a type of diagnostic testing(US), computed tomography

(CT), and magnetic resonance imaging (MRI) can be employed (Priyadarsini and Selvathi, 2012).

Threshold-based techniques, numerous inferential statistics, Ann models, distorted methodologies, clustering algorithms, and machines attempting to learn techniques have all been employed in the past for the separation of the liver territory and cancer treatment in the liver (Campadelli, 2009). Hand-crafted features with feature representation, connection, and connection are significantly used in traditional machine learning methodologies. The features extracted from the feature extraction method influence the classifier's efficiency. Lighting changes, image noise, lower brightness, diffraction and blurring are all issues that these systems face.

According to a 2006 assessment by the American Society of Clinical Oncology, liver cancer is the most fatal of the cancers (American Society of Clinical Oncology.2006). As a result, cancer, the world's largest sixth most common disease, kills one out of every three people (Joshi, 2013). Hepatic carcinoma is another name for liver tumor, and the most communal sign of liver cancer is hepatic cellular carcinoma (HCC) (American national society, 2016). Liver cancer is the unrestrained development of cells inside the liver. Tumors are divided into two types: cancerous and non-cancerous cells (Reddy, 2012). Every year, 12000 individuals die from liver cancer in the world. To prevent this, the problem must be examined at an early stage, as early discovery can enables doctors rescue lives while posing little health risk. (Sridharan, 2012).

Ultrasound, MRI, and CT are some of the technologies utilized to collect images of the liver from individuals, but CT is the most effective liver cancer diagnosis testing method. Hence Radiograph is widely employed in the field of medical advances. Therefore, sectioning a liver picture, removing liver lesions, and identifying a liver lesion are crucial because distinguishing among liver and non-liver tissues requires an expert physician (Alahmer, 2016). Even professional radiologists have indeed been known to overlook malignancies in their early stages due to malignancies that are imperceptible to the human eye.

In general, there have been several breakthroughs in imaging techniques, such as deep learning, image analysis, and machine intelligence, and skilled radiologists can apply these technologies (Belgherbi, 2013). Collaborating with a skilled ophthalmologist and hospital devices for laptop tests allows for proper characterization of a liver illness. Clinical assistance will be provided to doctors in order to improve diagnosis and update and maintain. This procedure safeguards the victim against the dangers of surgery and diagnostics.

Tumor extraction methods from CT scans of the liver are an important aspect of laptop surgery and disease diagnosis (Bhullar, 2014). Therefore, expert evaluation and early detection of liver cancer in the realm of medical radiography remains a considerable issue. In order to provide effective treatment to the patient, doctors must first determine the tumor's capabilities. Doctors can use this knowledge to make more informed decisions (Chung, 1998). Any general way of fully automated computer supported system will researchers and clinicians in offering efficient medicines by detecting the liver cancer characteristics (Zhou, 2012). Cancer of the liver, among other things is disease that originates in the liver fairly than in other structure and then spreads to the liver. In extra arguments, tumours that originate elsewhere and end up in the liver are not considered (primary) liver carcinoma. Primary liver malignancies are malignancies that begin in the liver.

(R.Rajagopal and colleagues, 2014) A new and precise technique for segregating liver tumours using computed tomography (CT) scans is described in this research. Pre-processing of the liver CT image comprises image contrast augmentation and removes noise. The author utilizes a vector support network (SVM) encoder that was learned using user-fed data sets to characterize the tumour position from liver imaging. To improve the SVM classification's rough segmented image, feature removals and morphology methods are performed successively to the fractured binaries image. The results of the experiments reveal that the algorithms are more productive and accurate than previous methods. The writer described a new method for autonomously fragmenting liver tumours from a CT scan of the hepatic as well as a validation study. The tumour segmentation method used in this study is a ground-breaking method for tumour categorization that supports health personnel in further diagnosis. Our technology's main benefit is that it offers accurate results for all types of liver tumours quickly without any need for human input. (Vijayarani and colleagues, 2015) in recent years, data analysis has become a common tool in the healthcare business for predictive modelling. Data is used to remove information from storage facilities, big records, and other sources. Academics face a severe challenge in forecasting disorders from large medical databases. To overcome this challenge, investigators use data mining techniques such as clustering, categorization, and clustering algorithms. The study's main purpose is to employ classification techniques to anticipate liver diseases. In this work, the Nave Bayes and SVM classifier approaches were used (SVM). These classifiers algorithms are evaluated using performance criteria such as classification results and processing time. The SVM is a better predictor for detecting liver problems, according with findings of the studies. A frequent data mining technique is categorization. The Nave Bayes and Support Vector Machine (SVM) classification methods were utilised in this work to forecast liver illness. These techniques are evaluated focusing on categorization and algorithm to classify performance measures. The SVM classifier is the preferred approach, according to the results of the studies, because it has the most advantages. When comparing response times, the Nave Classification algorithm, on the other hand, needs the minimum execution time.

The urgent requirement is for well-targeted algorithms that can deal with poor aberrations, grey scale inconsistencies, and fractured boundary while still generating good results. Algorithms and traditional procedures are unsuccessful in these scenarios. As a result, a more robust architecture is created to avoid excessive while also providing closed, continuous, greater segmentation, and improved location over time. As a result, in our enhanced watersheds technique, we offered updated and better watersheds methodology that eliminates the need of an unnecessary segmentation process. Likewise, we can improve the tool's efficiency in a practical scenario by employing the tool's SVM phenomenon predicting set. CT scans or MRI (Magnetic Resonance Imaging) pictures are used as they're more precise and offer better image results, enabling us to detect cancer lesions early. So it's tough to spot liver cancer in body structures because to the jumble of tissues and organs, SVM Phenomena helps our improved algorithm the with forecast approach.

An abdomen CT scan can reveal several body organs, as well as the liver. To extract the correct qualities of the liver, the liver portion of the CT scans must be divided. Active shape model and Laplacian mesh optimization (Assaf et al., 2016), Deep learning methods have already been utilized to distinguish the liver from abdominal CT images using Gabriel et al. (2016), graph cut technique (Guodong et al., 2015), and 3D liver segmentation (Zhang, 2017). For liver segmentation, unsupervised artificial neural networks have received a lot of attention, and they outperformed classical segmentation techniques. The conceptual liver extraction on stomach CT images was given using supervised Deep Adversarial Networking (DAN) and Weighted Loss Function (WLF) (Kaijian et al., 2019). Furthermore, the convolutional neural network (CNN) was used to separate lesion in liver CT images, which resulted in a similarity coefficient of 80.06 percent when it comes to dice (Wang et al., 2013). It has been discovered that combining a DL method with graph cut refinement improves the efficiency of liver CT image segmentation (Lu et al., 2017). In the graph-cut process, the forefront part of the liver is often considered as the forefront, while the backdrop part is widely regarded as the observed in the xrd architecture. Cut algorithms are then used to separate the surroundings and forefront objects into uniform pieces (Boykov and colleagues, 2001).

Density methods compare the grey luminance of a pixel to the luminance of surrounding pixels to estimate the patterning of the liver. The seeding spots are physically inserted in the parenchyma of the liver by the procedure's specialist. The images that match the implanted pixels are collected together just to create the homogenous textural zone. This was a tractor trailer system that relied on a manual training images for effectiveness. Lopez et al. (Lopez et al., 2013). Due to the lack of an effective method, brightness approaches focused on breaches in the carefully seeded region, ridges, rough, and angles. When working with MR images with a substantially diverse area, strength techniques have been found to be useless (Sharma and Agrawal, 2010).

Computer learning-based techniques such as support vector machines (SVMs) (Defeng et al., 2012) and regression trees (Norajitra et al., 2015) have been successfully described for quantitatively identifying characteristics from digital images. In terms of performance and discriminating, these systems surpassed density approaches. These methods often can result in leakage or coarse separation due to the rotation and disturbance. In order to get quantifiable characteristics instead of palm attributes, CNN has recently been suggested for liver separation. In a short length of time, it was able to separate heterogeneous liver texture (Elshaer, 2016).

With the use of multiple shallow and deep learning algorithms, different form, texture, and gradation based features have been retrieved for the diagnosis of liver cancer. For the diagnosis of liver cancer in unprocessed and non-pre-processed CT images, a computer-aided approach based on auto-covariance texture characteristics was described. The roughness of the liver texture image is captured using covariance-based features. The illumination changes, orientation, poor contrast, blur and size of the liver picture were all common problems with the region - based technique. Using the auto-covariance texture characteristics, the reliability was 81.7 percent (Huang et al., 2004). A particle swarm optimization (PSO) technique was utilized to detect hepatocellular carcinoma in liver radiography. PSO can provide a decent solution and determine the appropriate variables for a greater tumor detection rate when used in combination with other algorithms. PSO's performance may not be assured, and may become stuck in the localized optimum, necessitating additional learning repetitions. Instance optimization (IO) and SVM were found to be far more effective in detecting liver cancer. (Jiang et al., 2013)

Furthermore, an advantage spacing standardized level-set evaluation approach has been offered to divide the tumour, cyst, calculi, and healthy liver. Edge-based proximity was used to determine the link between the liver's shape and color. A multi-channel convolution neural network (MC-FCN) model has considerably improved the detection of liver fibrosis. Neural nets are an automatic learning method to increase regional representation of raw data and characterizing aggregate texture properties (Sun et al., 2017). Many statistical tools, such as the grey level co-occurrence matrix (GLCM), have been used to derive actual attributes. The GLCM has qualities including energy, correlations, volatility, and uniformity. The grey level brightness is an important factor in displaying CT scans of the liver, borders, and texture variations that are minor. It is simple to implement, stable, and durable for low data stores. GLCM-based algorithms have limited efficiency because to the requirement for user intervention, noisy, blur, brightness, and uneven illuminance of CT images. While the front or background is thinner, the platform's effectiveness suffers (Hu et al., 2018).

(Huang and colleagues, 2004) Huang used non-enhanced CT scans to illustrate a machine diagnosis approach for diagnosing and sectioning liver tumours. In their manage a large project, they used auto-covariance textural characteristics to identify the tumour with an accuracy of 81.7 percent. Using a particle swarm optimization technique, (Ji et al. 2014) proposed an effective computational formula for hepatocellular cancer clinical condition. A new and more efficient enhanced technique svm based and scenario modification has been proposed for the identification of hepatocellular carcinoma with improved results (IO). Using an advantage distance normalized level-set assessment process; Li correctly separated the cyst, calculi, tumour, and normal liver in CT images. A number of co deep convolution network (MC-FCN) model improves its efficiency in segregating liver cancers in CT scan images. The GLCM and other extracting features techniques are successfully submitted in machine learning approaches to distinguish evaluation measures.

The most frequent cancer in Asia is hepatocytes carcinoma, which can spread to other parts of the globe. The authors have focused on a segmentation technique that works well in a square ROI and uses two-level threshold method (Region of Interest). In additional, the liver's edges were identified using structural filtration. In furthermore, the borders have been adjusted so that the floodplain approach can be qualified. Finally, the specified area that you desire is built. Lim et al. (Lim et al., 2004).

Using watersheds techniques, feature extraction, and area combining processes, we can diagnosis liver disease more correctly and accurately. Therefore, Effective detection is highly challenging due to the intricate human tissue scrambling, anatomical features, and individual differences. Liu et al. (Liu et al., 2009).

Liver cancer is the most common cause of death from cancer. In practice, early detection and prediction of stage of disease are considered key aims. Or before, which includes an average filtration global histogram equalization; second, converting pictures into an intuitionistic fuzzy domain process, in which each reflects either Truth/False or Unquantified; and third, transforming images into an intuitionistic fuzzy url phase, where everyone represents whether Truth/False or Indeterminate, according to the writers. Finally, using this strategy, you can reach an efficiency of 90 per cent. (Sayed et al., 2015).

Liver cancer is the 3rd most fatal cancer in the world. It took the lives from around 70,000 people in 2008, accounting for about 9% of all cancer - related deaths. To identify cancer contours, the researchers use three critical procedures: first, image pre-processing; second, the watershed approach; and third, forecasting and training utilizing Support Vector Machine (SVM) depending on experiences and structural processes. Direct relationship, it proved to be highly exact and economical, as per the authors (Zhang et al., 2011).

1.2 Objectives

1. Apply enhanced watershed algorithm with SVM phenomena as an active detection tool for liver cancer?

2. Remove undetected lesions of liver cancer by using enhanced watershed algorithm and SVM phenomena?

3. Evaluate the efficiency of EWA (Enhanced Watershed Algorithm) with SVM against prior algorithm for liver cancer detection?

4. To know the level of undetected possibility of liver cancer with the present algorithms and EWA with SVM phenomena?

1.3 Practical and Scientific Applications

1. Awareness of liver cancer among society.

2. Provide a significant prediction model for improvement detection of liver cancer using a EWA with SVM phenomena.

3. Examine the parameters used to detect liver cancer. 4. Set a podium to predict liver cancer at earliest.

1.4 Hypothesis

H1: Patient and medical image researchers need to know about the EWA for detection on the basis of some prediction phenomena.

H2: Efficiency of proposed algorithm necessarily shows that the entire possible prediction framework are added and evaluated properly.

H3: EWA combined with SVM phenomena will be capable of detection of liver cancer efficiently and accurately.

1.5 Research Questions

1. How does the practical implication of the EWA with SVM phenomena affect the quality of liver cancer detection?

2. How does the practical implication of EWA with SVM phenomena reduce the probability of misdetection caused by complex human anatomy?

3. Can an effective EWA with SVM phenomena helps to reduce the probability of liver cancer?

4. What recommendations can be suggested for the medical image processing workers that can assist them in detecting liver cancer?

Chapter: 02

Literature Review

2.0 Introduction

Several researches have been presented to diagnosis various tumours or liver cancer using features extraction methodologies. A various densities was presented in (Song et al; 2013) for describing ridiculous surface data through the combination of multiresolution Gabor filters with template matching scatter plots for normal lung categorization. The authors of (Nugroho et al; 2019) presented a CAD system for malignant tumors that used internal and exterior factors to extract geometrical and textured elements. Furthermore, internal properties were classified using a convolutional network, whereas exterior features were classified using.

The numerous educations have presented article manufacturing approaches incorporated in CAD systems using CT scan images for liver cancer diagnosis (Chen et al; 2017). The region expanding procedure and fuzzy C-means (FCM) are common segmentation technologies that have been used extensively for either liver or lesion localization (Kumar et al; 2013) The preponderance of liver CAD systems have employed statistical characteristics to describe textures and form, such as GLCM features, wavelet coefficients counts, and quantitative techniques of mean, skewness, variance, sample variance, and kurtosis (Gunasundari et al; 2018). In this instance, the liver CAD system relies largely on feature extraction, which has a significant impact on overall efficiency. Traditional multiple regression analyses computer reinforcement learning, such as stochastic neural network models (Kumar et al; 2013), SVM, and linear regression, were used in the classification step (Chang et al; 2017).

Deep tools in the classroom have recently appeared in medicinal image segmentation employing a number of visual modalities. Deep education procedures have been studied for segmented, extraction of features, and categorization, which are the 3 most common things. For example, these methods have been extensively tested with a variety of anatomical structures. (Organs or bodily regions) for medical picture analysis, such as the chest (Cheng et al; 2017), prostate (Roussel et al; 2017), heart/cardiac, artery, thyroid, intravascular, foetal, lymph node, spine, bone, muscle, tongue (Roussel et al; 2017), and more. To complete these objectives, various types of deep networks have been used.

2.1 CNN models

The large percentage of works have been using CNN models to understand from imaging techniques and hierarchies esoteric characterizations, accompanied by a soft - max or other sequential classification algorithm (such as SVM) which is used to provide certain or more likelihoods or scores for government systems utilizing deep learning method in the prognosis of cancers (Yang et al ;2019), such as liver cancer, The impact of networking macro factors on performance overall has been overlooked in the vast of these studies. Until far, there have been few strategies to improve categorization, extraction of features, and conceptual framework of this study using common deep convolutional neural (Chitradevi et al; 2019)

Architectures, like most neural network models, are subject to issues like lack of hyper parameter adjustment, many local ecoboost, and increasing computing time. Management of the network architecture and hyper characteristics has become a critical effort in order to avoid these issues. In principle, microbially optimizing methods are widely used in optimization issues. (Beloufa et al; 2013) such as ultra - sonic echo prediction, cancer advancement mechanism genetic traits selection, affymetrix cancer categorization, Microarray technology categorization, retinal image translation, metagenomic data downsampling for classification tasks (Prasartvit et al; 2013), and mellitus diagnosis of diseases However, these methods have rarely been employed to improve the outcomes of CNN-based segment, extraction of features, and classification. As a result, the impact of combining several deep learning algorithms with microbially optimization on the segment, semantic segmentation, and classifying of liver lesions from CT images is investigated in this study.

Artificial intelligence's application in the realm of healthcare systems has substantially expanded in recent years. In the realm of clinical diagnosis, computer vision, as a post of intelligent machines, has numerous applications. Chronic illnesses are one of the most common illnesses on the planet, and simplifying and speeding up their identification will have a significant impact on their future therapy. (Lam et al., 2017) Used different machine learning algorithms, such as SVM, RF, and NB for position recognition, and the Smart Mind national healthcare system for motion sensors, to create an active notifications system that will monitor Alzheimer's clients (A. Norouzi et al; 2014). A neuromorphic algorithm was utilized to reliably assess medical data in order to diagnose main diseases and provide therapy for sufferers. 3 types of medical information were processed using statistical approaches such as decisions trees, NB, SVM, and the Optimization algorithm to construct forecasting model by extracting effective methods, which provided satisfactory results. (Leguizamón et al., 2016) developed a fuzzy system that is based on evolutionary algorithms to forecast the danger of cardiovascular syndrome, and simulated results demonstrated the presented product's good performance.

(Ramzan et al; 2020) conducted investigations for the diagnosis of cardiac diseases in healthcare situations The ANN algorithm has a 97 percent accuracy rate, the Cart method has an 87.6% correctness rate, and logistic deterioration has a 72 percent correctness rate. (Mr. Hongxu, YI N et al., 2017) A multilevel fitness management information system for the correct identification of a number of conditions such as arrhythmias (86%), type 2 diabetes (78%), urinary bladder problems (99%), kidney stones (94%), and hyperthyroidism (95%). (Mr. Yip et al; 2017) used computer vision to construct and validate a model results of laboratory variables to detect and forecast liver problems in the overall population. Then, (Tingtingzhao1 et al., 2017) employed correlation matrix to come up with a solution Researchers employed neural networks to forecast diseases regarding medical histories and the in teaching strategy to forecast the risk of numerous diseases in a 2017 study (Zhang, J. et al; 2017 ; Mr. Tripoliti et al., 2017) provided an automated strategy for timely identification of class alterations in patients with heart disaster utilizing sorting methods with the maximum effect size of 97.87.67 percent, correspondingly. (Mr. Kim et al., 2017) utilized a mechanism education technique to categorize depression condition and treatment group using microarray examination of blood and heart currency fluctuations to discover indicators of the changed surroundings (Mr. Kim, et al., 2017). The preceding techniques' effectiveness has been to make a diagnosis these problems.

Mr. Lee et al. (2017) suggested a technique for identifying faulty electronics oscillations based on transplantation parameters for accurate cardiac diagnostic techniques in a 2017 study (Mr. Lee et al.2017). The precision of unusual sound wave harvesting was tested exhausting real ECG data for a healthy individual and a physician with myocardial injury in this test, and the outcomes demonstrate that the suggested method can not only adequately interrupt the unusual waveform but also provide a thorough examination. (Mr. Dominguez-Morales et al., 2017) used the Newomorphic Hearing Sensor for FPGA to develop a convolutional neural internet tool for identifying healthy and psychopathically unwell people Decomposition of audio. The best quantity is 97.05 percent, and the worst scenario is 80 percent, based on this method and varied quantities. Machine learning algorithms were utilized in the study of (Mr. Timothy et al.2016) to mechanically identifies different ailments depending on heart rate fluctuations. The technique of analyzing data input via ECG recording has attained a high level of precision. Mr. Ekz et al. (2017) employed and compared six approaches of various learning methods to identify cardiovascular disease in MATLAB and Veka surroundings, including linear SVM, two-way SVM, percussionist SVM, transitional SVM, transitional SVM Gauss, and the logistic regression.

(Mr. Gagnon et al; 2017) then created a wireless electrocardiographic recording device that uses an electrodes to monitor and store the heart's ECG system and is linked to a sample via a reduced wifi connection by a host machine. It is ensured that ECG data can be retrieved and shown in live time for quick examination. SVM, stochastic forest, and multilayer perceptron are three computer training algorithms that were built using ECG data to proactively vaporise the heart of heart patients from the physiologic brain. Learning strategies for modelling in the shape of a two-layer neural net to forecast wait period as 1-wait 2-link and 3-dead at three different time periods of 180.365 and 730 days are described.

(Mr. Luo, Y et al.2017) investigate a method based on heart MRI, which is an active data gathering imaging methodology that employs left cardiac MRI to measure heart muscle, ischemic stroke, and features. It is critical that aspects such as partition program and width work well. Machine learning approaches for assessing medicinal pictures with approximations of more complicated models utilising exercise data were explored in this strategy, which is a suggested fast, reliable, effective, and appropriate method for LV splitting. From Cart tree reversion cataloging to build an analytical strategy for disease diagnosis using data mining algorithms From the Cart method to rule discovery, fuzzy rules based on the EM algorithm for data sorting To decrease features and cope with the globalized issue in data, the Pca algorithm that uses fuzzy regulation techniques for forecasting.

(Mr. Ali, B et al. 2017) proposed artificial neural network (ANN and Bayesian networks as machines learning strategies for identifying insulin and cardiovascular problems. The goal of this resource is to learn about convolutional neural networks and Density estimation, as well as how they can be used in categorization. Diabetes and cardiovascular are being studied to see whether machine learning algorithms produce the best categorization results. Artificial neural network (ANN) and evolutionary operators to accurately identify heart problems; it shows a highly hybrid technique for the identification of cardiovascular disease with correctness, sensitivities, and selectivity of 93.85%, 97.5%, and 92.5% in the Z-Alizadeh Sani dataset. Heart failure has been offered as an Enseble-based method for creating new designs by integrating posterior probability or estimated values from numerous earlier models to generate more efficient methods that identify 89.01 percent of tests using data from the Heart Collection directory. Cleveland was recovered, and its specific specificity and sensitivity in the detection of cardiac disorders were 95.95 percent and 91.95 percent, accordingly.

(Vaishnavee et al; 2015) used SVM and self-organizing Map (SOM) techniques to solve the problem of brain tumour segmentation. In the also before the stage, histogram equalization was performed. The mean, severity, number of episodes, and variation were found to be the four components to be categorized. In the second phase, they used SOM grouping to locate and divide the uneven brain regions. In addition, brain MR pictures were divided into based on inters groupings. A Principle Component Analysis (PCA) was employed to evaluate these texture features in semi levels in order to demeanor this classification of the grey level founder texturing matrices. However, the authors did not compare results in state of art and there was no explanation for spending SVM and SOM.

2.2 SVM Technique used in Brain Tumour

For the division of brain tumours, (Arikan et al. 2016) suggested a moderately, crowd sourced seed collection SVM technique. To remove noise from MR images, they used a gaussian filter as during or before stage. From the conventional MR images, unique samples would be picked for the SVM classification. A freely available BRATS 2015 database was utilized to assess performance. They chose four individuals from the MICCIA BRATS-2015 statistics gathering to examine the novel procedure's results. In comparison to the underlying reality, their approach had an regular Dice Similarity (DS) of around 81 percent. (Ellwaa et al., 2016) suggested a completely automated system the recurrent randomized tree is used in a segmentation strategy for MRI-based brain tumours. Recursively, the child's accuracy with precise information in the statistics set utilized for randomized forestry categorization was improved. The method was put to the test at BRATS-2016. Collection criteria for the person with the most experience lead to optimistic results. However, no reason for the selection criteria was offered, and no reliability results were reported. On the BRATS 2013 dataset, (Abbasi et al; 2017) presented a 3D mechanized platform for brain tumour sorting and segmentation. ROIs (Region of Interests) are segregated from the FPGA for well before, inhomogeneity rectification, and summary transmission. Though, they recycled artificial facts for experimentations and described an accurateness of 93%.

(Mehmood et al. 2019) planned an efficient MR-based organization for neuroimaging and modeling. The brain and tumour regions are fundamentally separated from the MR sections using an immersion, tractor trailer 3D segmented method that uses SVM 95.53 percent correctness, 99.49 percent compassion, 99.0 percent resolution, and 0.09 root mean square. Studies on identity information, on the other hand. Using mouth feel features, distinguish between normal and diseased tissue samples. GMCH, Guwahati Hospitals provided 80 photos of aberrant and normal tissue for this study. Five descriptor (LBP, Tamura, HOG, GRLN, and GLCM) were combined to collect features from an image, yielding a set of 172 able to highlight. SVM, K-NN, Linear Regression, Polynomial Factor analysis, and Linear Discriminant are among the six classifiers used to assess the presentation of each set of features in both group and separately. The investigational findings showed that employing the entire feature set improved the overall classification accuracy to 98.6 percent when compared to using separate feature sets. They came to the conclusion that the computer-assisted technique could lead to more accurate analysis, as adolescent brain injuries are extremely dangerous. The system is slow and computationally intensive due to the employment from several classifications.

From Medical Behaviour, (Iqbal et al. 2019) suggested a deep convolutional neural network for reliable brain tumour identification using co - evolutionary machine learning with short attention span (LSTM) (ConvNet). Convolution and LSTM are two alternative models and use the same set of data to generate a group and maximize performance. The two distinct models are combined. For this purpose, a data set containing MRI images in four probes (T1, T2, T1c, and FLAIR) is publicly available. MICCAI BRATS 2015 is now available for viewing. Various changes are constructed, and effectiveness of the product modifications is applied to the processing procedures, such as noise removal, histogram equalization, and edge detection, to improve image quality. To address the problem of class disparity, contemporary models employ class loading. The trained model is checked for verification details from the very same image capture, and the results of each operation are stored. ConvNet has a single score (exactitude) of 75 percent, whereas an LSTM-based network produces 80 percent, for a total merger of 82.29 percent. (Saba et al; 2020) is used to segment real-life loss indicators, while the Special Interest Domain Adaptation System (VGG-19) is finished to generate features that are then constructed (form and texture) in a sequence. Entropy built such capabilities to consistently and quickly recognize and deliver fusion variables to categorization units. The proposed approach is put to the test in the MICCAI competition data, 2016 and 2017, using cutting-edge scientific picture processing and laptop treatment, accordingly. The study found that utilizing 2015 BRATS, the coefficient of dice similarly (DSC) was 0.99, 1.00 in 2016, and 0.99 in 2017. They did not, however, test the efficacy of their method using other classifications or their merger.

Lately, (Ramzan et al. 2020) used 3DCNN with residual connections and substantial convolution to successfully forewarn later part mappings among MRI dimensions and spatial brain sections. Using data from three distinct sources, mean dice scores of 0.879 and 0.914 were calculated for three and nine brain areas, correspondingly. In contrast, an average dice score of 0.903 was achieved for 8 areas of the brain with MRBrains18 data gathering, which is greater than the 0.876 acquired in the previous study. Similarly, (Nayak et al. 2020) suggested a CNN model consisted of 5 levels (four Convolutional and one completely layer) with training examples to identify neurological symptoms through MR image analysis. Two benchmark inter brain MRI samples, MD-1 and MD-2, were used to test the validity of their approach. On the MD-1 and MD-2 datasets, the researchers stated categorization accuracy of 100 percent and 97.50 percent, correspondingly.

(Lu et al. 2020) proposed a profound understanding Gliomas categorization using CNN ResNet based on pyramids dilated compression. Studies on a local big dataset yielded an accuracy of 80.11 percent in glioma identification. They did not, nevertheless, employ a standard database in their trials.

(Setio et al. 2016) proposed a multi-view Quaternion network was utilized for training the model in a method for identifying Respiratory Nodule. For accurate determination of all worrisome lesions, three techniques were merged for potential skin lesion segmentation: sizable, inter - and intra, and substantial. On the publicly released LIDC-IDRI database, the suggested system is trained and verified. The research work obtained a detection threshold of 85.4 percent at 1 falsified and 90.1 percent at 4 false-positives. Using 3-DCNNs from dimensional CT scans, a new method for reducing false-positives in automatic tumor detection has been developed. This method was thoroughly tested in the LUNA16 competition, where they earned the greatest CPM score while reducing the completely untrue tracks.

(Shen et al. 2017) launched a new based image classification scheme with lower and higher concern levels. Employing a recent multi-crop pooled strategies to maximize relevant knowledge from nodules by removing areas from sectorial features mapping and using maximum pooled times, the inter convolutionary neural networks is employed for this approach. With the LIDC-IDRI data, they were able to get a good 87.14 percent arrangement performance and 0.93 percent CUP counting. The classification of microscopic images in order to determine whether they are cancerous or harmless. They secondhand openly accessible LIDC data records cohort, a Python programme, and to supply 3D slicer front-end code a method for measuring 3D aortic lumen dimensions from a greater focus using a simple iterative model. The suggested individual's tests for a mean DSC of 0.951 have always been higher than 0.928 in entire datasets and assessed 3D sections of 16 CT cases. The median spacing between the 16 cases is a little less than 0.9 mm. The proposed solution is extremely accurate, and an elevated result might be reached in both rare and common scenarios. Consequently, the investigational setup working was not clearly clarified and results were not associated in the state of art.

2.3 CNN Technique used in Lung

(Xie et al, 2019) To enhance the CT reading ability, researchers presented a novel automated Detection of pulmonary nodules using a 2D neural Convolutional Neural Network (CNN).. To begin, modify the Faster R-CNN setup to identify nodule possibilities using two area proposition systems and a background subtraction layer with 3 copies for three types of slices for final result mixture. Another, a new 2D CNN structural design is being developed to attain high wrong removal, which is a classifier that distinguishes between genuine nodules and possibilities. A sequence that increases sensitivity to lung nodules recognition for the retraining phase. Lastly, the exams are combined in order to poll on the firm's official outcome. LUNA16 performs comprehensive testing with a specificity of 86.42 percent. The falsified decrease efficiency at 1/8 and 1/2 FPs/scan is 73.4 percent and 74.4 percent, correspondingly. The suggested method proved that based image recognition could be done accurately. The claimed precision, on the other hand, is not up to par with the top of the line.

(Jiang et al. 2018) proposed that inter cut out of the Frangi tube's lung image may be used to successfully identify fundus images. A four-channel neuromorphic model that integrates two excellent illustrations to gather physicians' feedback for the diagnosis of tumours from 4 levels. With a 94 percent sensitivity of 15.1 fictional ones per sample, 80.06 percent of the sensitivity could be attained for the fourth false-positives for each scan. They found that using the patch-based learning method in many groups improves performance and reduces false-positives considerably in vast amounts of visual information.

(Naqi et al. 2018) suggested four central steps make up the nodular method of detection and diagnosis. First and foremost, the lung region is abstracted using the optimal dark established using Evolutionary particles minimization. Then, in a parametric system, a new strategy for identifying candidates is presented, which is centered on the geographical healthiness of the clusters. In the subsequent stage, a amalgam geometrical consistency descriptor was formed to improved depict the nominated nodule, including both 2D and 3D information about colony candidates. In conclusion, a profound solving situation to the false-positive consequences was proposed, focusing on Softmax and the stacking auto encoder The Lung Image Database Cooperation and the Data Repository Networking Initiative, the largest publicly available publicly useable collection, reveal that the proposed strategy reduced false-positive rates to 2.8 per scan, with 95.6 percent sensitivity. A method for automatically identifying nodules and classifying them. The Active Contour Model (ACM), 3D neighbourhood connectivity, and the regulations on geographical features are all part of a current 3D nodule hybrid sensing method.

A hybrid extracted features is produced using a Pr by combining geometric texturing with the Color Feature Probability (PCA) for each cluster contender. Four different classifiers are used to sort the data: Naive Bayesian, Support Vector Machine (SVM), and Logistic regression. After the abstractions phase is terminated, 4 distinct classes are introduced. The test is carried out on a subset of the Dataset Coalition's members (LIDC). AdaBoost outperformed all other classifications in order to develop correctness, sensitivity, sensitivity, and scan. Moreover, the method of (Naqi et al. 2019) is computationally exclusive and requires multiple assets, and the reliability is not greater than other approaches published in the state - of - theart.

(Asuntha et al; 2020) Using HoG, WT, LBP, SIFT, and Zernike Moments for aspect removal, a deep learning technique for the diagnosis of computed tomography was given. Following removal, the Fuzzy Particle Swarm Optimization (FPSO) technique is used to render the favorite asset. In the end, dark suede is employed to define these qualities. A modern FPSOCNN reduces the computational complexity of CNN. On the LIDC-IDRI dataset, the shows a detailed evaluation of existing computer - aided diagnosis technologies. There are four key phases to an computerized system for tumor subdivision detection and arrangement. Pre - processing stage, classification, extraction and classification, and potential lesion identification are all steps in the process And use a k-fold cross-validation technique, and elected autoencoder for lung nodule categorization, they achieved 100% reliability on the LIDC information.

(Premaladha et al, 2016) developed an intelligent method for accurate melanoma categorization and prediction. For picture improvement, the segmentation method and Contrast - Limited Adaptive Redistribution approaches were applied. To isolated the lesion from the casing, a new subdivision method (Normalized Otsu's Morphology) was applied. As a result, the problem of fluctuating illumination was reduced. Fifteen characteristics were retrieved from the segmentation results and supplied into the suggested classification (Paying close attention neural network models with hybrid Classifiers). The system was evaluated and confirmed with over 992 photos of nonthreatening and malevolent tumours, and it obtained an exactness of classification of 93 percent.

(Bareiro Paniagua et al. 2016) The approach uses a Dermoscopy image to determine if the lesion is cancerous or harmless. This process contains of the subsequent modules: picture preparation, lesion delineation, semantic segmentation from a disease, and categorization. Remove undesirable elements, such as hairs, during the pre-processing stage. The ABCD rule was used to retrieve features from the impacted regions that had previously been divided. Lastly, using Classification Technique, lesions were categorized as normal and cancerous (SVM). On a dataset of 104 Features extracted, investigational consequences showed that the concept has an efficiency of 90.63 percent, a sensitive of 95 percent, and a specificity of 83.33 percent. As far as diagnosing performance goes, these results are very promising.

(Khan et al. 2019) Using texture and colour elements that are commonly used in image processing the majority of these solutions used handcrafted characteristics, which reduced the efficiency of computer frameworks. Similarly, Aima and Sharma [95] use CNN to diagnose early phase melanoma skin cancer using 514 morphologic pictures from the ISIC dataset. They had 74.76 percent accuracy and a 57.56 percent validation loss. Dai et al. [96] suggested a CNN model with pre-trained 10,015 skin cancer photos using a cellphone as the inferences platform. All computations for testing a new source were done locally, where the test results was saved. Their solution, on the other hand, reduced latency, saved electricity, and increased efficiency. The observed reliability is significantly lower than what has been published in the research. A deep convolutional neural network (DCNN) is used in three steps to detect and recognize skin lesions: results were compared, lesion border collection, as well as in characteristics retrieval. An entropy technique was used to select discriminating features. The suggested approach is demonstrated on the PH2, ISBI 2016, and ISBI 2017 databases, while the identification phase is appraised on the PH2 and ISIC 2017 sets of data. The authors claimed that their approach outperformed previous methods by 98.4 percent on the PH2 dataset, 95.1 percent on the ISBI piece of data, and 94.8 percent on the ISBI 2017 set of data.

(Patel et al, 2015) proposed a method for detecting leukaemia at an early stage that is automated they developed a few filtering techniques (zack, histogram alignment, and k-state grouping) and used SVM to classify the data. The suggested system was positively built in MATLAB, and 93.57 percent accurateness was achieved. They did, however, conduct trials on a tiny dataset.

(Zhang et al. 2020) based on 5000 photos taken from a local hospital, used three ways to analyses the influence of the leukocyte classification First, with 94.23 percent specificities, 95.10 percent sensitivity, and 94.41 percent accuracy, CNN apps were used as the SVM input for leukocyte categorization. Using the HOG features in the SVM software, we were able to get 87.50 percent responsiveness and 85 percent accuracy. The basic features CNN and HOG were implemented with 94.57 percent, 96.11 percent, and 95.93 percent exactness, respectively. They did not, however, evaluate fallouts in terms of state of the art. In colored myeloid pictures, ALL subtypes and responsive marrow are seen. They introduced ST separation and used convolution neural network and machine learning approaches to fit the classifier on stem cells pictures.

2.4 CNN Techniques used in Liver Cancer

The majority of researchers employed computer vision techniques to detect liver cancers. Form, shape, and kinetic curves are three features exploited by automated processes that use multiple-step CT images. (Hamm et al. 2019) employed CNN design and multi-phasic MRI to develop an combined method for CT image segment accidents that centred on CNNs. The researchers compared CNN models to typical contrivance knowledge techniques such as

AdaBoost, RF, and SVM. The mean, variability, and contextual features were all taken into account when creating these categories. The mean frequency of dice compares accuracy, and warnings, correspondingly, were 80.06 percent 1.63 percent, 82.67 percent 1.43 percent, and 84.34 percent 1.61 percent. The data indicate that the CNN technique outperforms other techniques and is potential for liver tumour segmentation. AdaBoos, RF, and SVM effectiveness and distinction were tested on a small dataset.

A BoVW technique was proposed to characterize Focal Liver Injuries (FLLs) (Xu et al, 2018). In nine texturing sets, the area of concern (ROI) pixels was specified using the rotational motion invariant standardized local binary pattern system. As a result, a technique for expressing spatial cone matching is required (SCM) introduced to clarify the visual terminology of the ROI's geographic features To optimize the effectiveness of CNN for the categorization of medical images, Frid-Adar et al., [130] proposed using newly introduced deeper learning algorithms for artificial medical image creation (GAN). The proposed approach was shown using a small data set of 182 CT scans of liver lesions. For the first time, GAN structures were utilized to create high-quality ROI liver lesions. Then, using CNN, a novel method for diagnosing liver lesions was established. The accuracy of categorization using traditional data methods was 78.6% sensitivity and 88.4% accuracy. The findings improved to 85.7% responsiveness and 92.4% accuracy after incorporating the synthesized data rise.

(Romero et al. 2019) offered an end-to-end deep learning method for distinguishing recurrent liver tumors from benign cysts in CT scans of the liver. The residual ties and pre-trained Image Net weights are used in association with the efficient extractor function InceptionV3 in this method. To develop a probabilistic lesion type generation, the design also includes entirely linked categorization layers. They employed 230 liver lesions from 63 individuals from an in-house medical bio bank. Without disclosing the experimental setting or the benchmark dataset used, the reliability 0.96 percent and F1 0.92 percent were stated. The method for eliminating contrast proposed by PET/CT and MRI gray level histogram and gray-level co-occurring of liver lesions. A feasible and effective strategy to enhance the identification and characterization of FDG PET / CT and FDG liver damages that remain indeterminate after liver RMI / CT. (Jansen et al. 2019)used external factors such as the involvement of steatosis, cirrhosis, reported primary tumor that identified as characteristics. Fifty ANOVA F-score attributes have been picked and fed to a rather random tree grouping. The classifier testing was performed using the leave-out theory and ROC (ROC) curve study. (Ben-Cohen and Greenspan et al, 2020) developed a current way to construct realistic PET images by using CT scans, merging the FCN with a GAN to build digital PET information from various CT knowledge, which demonstrates its benefit by its completely bogus rate.

There has been a lot of study done on liver and liver tumour segmentation using moderately, computerized, and manually methodologies (M. Mharib et al ;2012)While detection and segmentation depends on specific sections or areas of the liver, hemi-liver, or vessels, semi-automatic and automatic techniques concentrate on various computer-based algorithms to accommodate liver or tumour edge detection from ct scans with quite some or no human input (S. Luo et al; 2014). To distinguish the liver or tumour from the rest of the body, a specialist or physician must always be present. Medical photos, either manually (with full involvement) or semi-automatically (partial involvement). The sections that follow include an overview of the existing literature or related projects in the topic of liver and tumour segmentation.

2.5 General Computer Aided System Approach

Computerized analysis is used in a broad Computer Aided Diagnosis (CAD) System to discover and define anomalies in medical pictures. These analyses are based on specific procedures or approaches, and they assist radiologists or doctors in detecting lesions, determining the extent of infection, and making diagnoses. CAD systems have been used to solve a variety of diagnostic difficulties in various imaging modalities such as CT, MRI, and ultrasound (N. Petrick et al; 2013). To aid medical workers in making decisions, image analysis, machine learning, pattern recognition, arithmetic, Artificial Intelligence (AI) technologies, and analytics are all merged into the CAD system.

2.5.1 Image Pre-Processing

Every medical image analysis approach uses image pre-processing to increase the quality of the material input image. It comprises noise reduction, enhancement, normalisation, and standardisation techniques, among other things. As identifying blocks and extraction of features are all based on image quality, pre-processing is critical to the success of subsequent phases. The normalisation and distribution techniques alter the image's values and restrict the spectrum, making it easier to optimise the class. Noise removal improves image graphical fidelity and removes superfluous values in the image, making other systematically planned such as border detection and object detection more successful, compression or segmentation Two strategies for eliminating noise from current medical imaging are the image pixels methodology and the digital signal processing approach.

Some examples of spatial domain approaches are mean screening, adjustable mean filtering, order-statistic filtration, adaptive weighed median filtering, Highest an inference filtering, Dynamical diffusion, Geometric Filtering, and so on. Each pixel in mean filtering is transformed by the average value of its neighbours. It gives the image a softening and blurring affect (H. Hwang et al; 1995). Local image characteristics such as mean, variation, and association are employed in the adaptable mean filtering method to discover anomalies and keep edges and features in tact (Goshtasby et al; 2008). Noise is reduced by using a local mean value to replace it. This type of filter adapts to the image's attributes locally and aids in the selective reduction of noise from various areas of the image (Pitas et al; 1992). When the sampling distribution has a substantial tail, order-statistic screens are particularly useful for decreasing noise. In comparison to mean filter, proposed technique is an Order-statistic filter that generates less blur and preserves edge clarity. By maximising Bayes theorem (Rekeczky et al; 1998), a highest probability filter is utilised to estimate an unseen signal. It is necessary to have prior knowledge about the image's probability distribution function in order to use it. Geometrical Filtering minimises noise while maintaining significant facts. It employs a non-linear, iterative algorithm to adjust the value of nearby pixels based on their relative value (Rahman et al; 2013).

Spectral domain approaches include the Discrete Wavelet Transform (DWT), wavelet shrinkage, wavelet filtering and diffusing, and curvelet Transform. Because DWT is strong at energy compression, the tiny and big coefficients in DWT are more likely to reflect noise and image size, correspondingly. Because these ten variables, which describe traits, are consistent across scales, they form geographically DWT provides an appealing base for de - noising since it creates linked clusters within each sub-band. Wavelet shrinking suppresses noise components while preserving visual feature values by setting a cutoff for wavelet coefficients. It's usually done with either soft or hard median filter, and it necessitates prior understanding of wavelet component stats. Weiner filtering is a wavelet based filter deployed to the wavelet domain that outperforms wavelet threshold method. Curvelet transform is a multi-scale conversion with scale and location attributes indexed frame elements. It has directed characteristics and a curvelet pyramids with high degree of freedom parts. Cuvelets are also used for noise reduction from medical images (Hilts et al; 2008).

2.5.2 Defining Region of Interest

The separation process, the target region or item of attention from the entire background in preparation for extracting features is known as determining region of interest (ROI). Both manually and semi-automated methods, as well as a planned activity, can be used to determine ROI in ct scans. Manual or semi-automated procedures necessitate user participation, but fully automatic systems do not. In most cases, a rough segmentation method is used to determine ROI in medical pictures. Thresholding, area expansion and border monitoring, classifier approaches, flexible models, and classification techniques are some of the common ways for defining ROI. Thresholding is the process of determining an average power To distinguish the intended object from its background, use either a local or global approach. It commonly divides pixels into two classes, one for pixels with a specific range of brightness and the other for pixels with a wider range of intensity. But it is a simple and effective method, and has its own drawbacks, including the incapacity to account for image spatial features, noise susceptibility, and intensity inhomogeneity. Region growth extracts related parts of an image depending on 11 predetermined conditions, such as intensity, picture feature, and so on (Godsill et al; 2008). It starts at a location called the seed point and ends when it reaches the ending criterion.

Labels are used in classifier algorithms to partition the feature space into separate groups based on tissue or anatomical location. Supervised classifiers employ better segmentation information as training examples, which is then used as a reference for segmentation and classification of fresh data. Unmonitored learners use grouping approaches and perform the same functions as classification method without the need for training examples. Deformable methods identify area borders using a sealed parameterized surfaces that changes or flexes in response to the model's internal pressure and the image's external factor. There are two types of deformable models: metric deformable models and geometrical deformation models. Organs are segmented using the Atlas guided approach, which uses information about the anatomical structure Atlas of Anatomy is a book of relevance. The atlas images are converted to actual pictures using linear, non-linear, or a mixture of linear and non-linear modifications, and segmentation is focused with finding likeness between two objects of comparable objects. Only when the patterns are similar across slices is this strategy effective (Kota et al; 2011).

2.5.3 Feature Extractor and Selection

Feature extractors are used to detect and choose differentiating and describing suitable for a variety from medical data in order to make decisions about a tissue's pathophysiology. The extraction of features can be done in both the spatial and spectral domains. It is always necessary to pick discriminating features after obtaining a big feature set. There are many features that may be derived from medical images, but texture-based characteristics are employed for learning a classification or automated liver or tumour segmentation. Texture analysis provides a wealth of visual data and is an important part of picture assessment (Adams et al; 1994).

Textural characteristics can be extracted using statistical techniques, structurally techniques, model-based methodologies, and transform12 based techniques. One of the most extensively used statistical methods for features extraction is the Gray Level Co-occurrence Matrix (GLCM), which is based on second-order averages of grey scale picture histograms (Pham et al; 2000). Another sort of statistical approach that leverages higher-order characteristics of the grey level histogram is the run length matrices. Texture is defined by structural approaches as a collection of very well texture components. A few of the structural model methods include from using various shapes of structuring elements to deformed versions of ideal texturing using real texturing. In model-based approaches, each pixel in an image is given a modeling approach based on the weighted estimate of the image intensity in its vicinity. Model-based methods include autoregressive models, hidden markov fields, and fractal models, to name a few. To extract textural information, transform-based algorithms work in the frequency response. Different image features can be extracted using a variety of bandpass filter, selected filter, or filter banks, and these characteristics can then be used for further categorization or segmentation. Texture analysis is an effective statistical tool for distinguishing psychopathically distinct regions in clinical When it comes to distinguishing specific types of texture, photographs have been shown to outperform sensory perceptions. (Pham et al; 20009).

2.5.4 Classification

The procedure of splitting a given object into various classes is known as categorization. The categorization phase divides the retrieved and chosen characteristics from the previous step into categories. Both unsupervised and supervised categorization are possible. The extracted features are categorized into predetermined categories in the supervised technique, whereas the feature sets are allocated to incomplete data in the unsupervised manner. To train and assess the classifier performance, it always needs labeled training data. Data for mri images training is often gathered from one or more specialists who have labelled a group of items.

Some of the categories include decision tree classifiers, minimum distance classifiers, closest neighbour classifiers, naive bayes classifiers, artificial neural networks, Support Vector Machine (SVM) classifiers, Random Forest (RF) classifiers, and Deep Neural Network (DNN) classifiers. A simple data structure with termination and non-terminal branches is used to create a classification tree classifier (Leondes et al; 2005). The terminal node indicates decision outcomes, while the non-terminal nodes represent one or more qualities. It's a supervised nonparametric teaching method used for classification and prediction. The data is divided into non-terminal branches using thresholds connected with characteristics until it approaches the terminal node. Decision tree algorithm are simple and quick to use, and they don't require much data preprocessing. In multi-feature space, a minimum distance classifier aims to reduce the space among unidentified visual information and the class. The gap provides a similarity measure, with the lower the index value, the greater the familiarity. This approach frequently use Euclidean distance, Normalized Euclidean distance, and Mahalanobis distance. The classifier Nearby Neighbors is a specific example classifier. It assigns the same label to the unidentified instance as the closest located neighbour in multidimensional space. They have a significant vulnerability to noise in training examples due to their strong focusing on the areas. The Naive Bayes classifier is a neural network-based classifier that uses the Bayesian technique to regularise the training phase. The Bayesian technique is based on the Bayes theorem premise. The sequential organization of the mind in information processing and the role of responsive physiological development is imitated by the Artificial Neural Network (ANN) (Gadkari et al; 2004). A self-learning network made up of statistical equations is known as an ANN. It is made up of three layers: an input layer, a hidden units, and an output units, each of which is made up of neurons. Backpropagation neural networks, multi-layer perceptrons, Hopfield networks, Radial basis function systems, Integrated regression neural nets, Self-organizing mappings, and other types of ANNs are among the many available.

2.6 Liver Segmentation

The process of segmenting a medical picture (CT, MRI, or US) into hepatic cells and non-liver tissue regions is known as liver segmentation. Structural equation models, graph cuts, clustering, deformable models, region growth, level set, thresholding, active contour, support vector machine (SVM), neural network (NN), and other techniques are used to divide the liver. A huge number of fully connected networks have subsequently been constructed, and they appear to be potential, but they demand a large amount of training data and an elevated CPU, making them extremely difficult.

Pohle et al. suggested a method for automatically creating adapting regions. By understanding the homogeneous aspect of the area, the liver can be segmented (Galloway et al; 1975). When the target is non-uniform, this approach performs under-segmentation since it relies on tissue uniformity requirements. For region growing, Kumar et al. used the centroid of the biggest linked region of the degraded image as the first seed point. They then used a Gaussian framework to compute the region's growth threshold, accompanied by post-processing to close the hole and link it to nearby tissues. Suzuki et al. developed a fully automatic approach for calculating liver size using the geometric segmentation method and the high speed level set The Fast marching level was used to generate a rough segmented at first, and the latter technique was utilised to improve the first estimate. There are several methods for achieving first rough categorization, such using fuzzy's level set algorithm or using the segmented image of one cut as a preliminary segmentation for a neighbouring slice. offered an optimised level set technique that used a multi-growth strategy, multi-curvature, and a finer resolution step 15 to change the model parameters in all stages of the procedure (Julesz et al, 1975) comprehensive adjustment at the last multi-resolution level Network cuts approaches treat the image as an unguided weighted network, with each node representing a pixel and edges connecting two nearby pixels.

Fast walking and classification techniques, statistics automatic threshold introduction, and k-means clustering were used to provide a fully automatic technique for liver segmentation with graph cut.

Because of the poor contrast between the liver and nearby tissues, threshold-based approaches are too harsh to yield an acceptable result for liver segmentation. However, it is occasionally employed as a first step in the rough segmentation of the liver or tumour. Clustering-based approaches are founded on the idea that in n-dimensional feature map, the separation and similarities among samples as compared to the same class are short and strong, accordingly. The approaches based on clustering are entirely automated and can execute several segmentations. Fuzzy c-means (FCM) and k-means clusters are commonly used in these strategies. Lu et al. and Zhao et al. used to achieve initial segmentation, which was later smoothed out via procedures and methodologies. When compared to K-means, FCM is more effective in entirely segmenting the liver and may also be used to modify the rough segmentation. The earliest active border was defined by contour using K-means (Safavian et al; 1991). Other clustering algorithms for MR images include agglomerative hierarchical segmentation and self-organized map. Masuda et al. clustered liver tissue using EM/MPM clustering. Both voxel intensities and surrounding voxel labels were employed in this strategy. The assumption behind structure-based techniques is that the architecture of a desired or interesting part of an object repeats in mathematics. For medicinal applications, these approaches have proven to be potent and successful. Structured based approaches for liver segmentation include flexible models, structural equation designs, and probability atlases. The capacity of SSM to restrict segmentation to roughly match previously seen for liver 16 segmentation, the shape of the training data is commonly used. Erdt et al. suggested a new SSM based on the local form priors mixed with constraints basically extracted from the designer's current curvature for fully automatic CT liver segmentation (Jain et al; 1996). This technique limits adaptations to areas where large conformational changes are detected and anticipated, resulting in a more robust system with less spillover to other tissues.

Texture-based approaches are the technique we used in our dissertation for liver segmentation. These approaches differ from previous segmentation methods in that they focus on texture rather than border. In generally, the texture-based technique has There are three significant steps. The first step entails obtaining texture information from the target object. Step 2 entails employing a classifier to assign these characteristics to a class, and phase 3 entails a post-processing step to refine and relax the region of interest. Huang et al. used neighbourhood mean, neighbourhood variance, Laws texture, and Unsers sum-and-difference scatterplots to derive four characteristics from a liver CT picture. Wavelet coefficients were utilised by Luo et al. to extract textural features from the liver and its surrounding tissues (Pohle et al; 2001). SVM was employed as a classifier in this strategy. Luo et al. published yet another study that used high-order statistical methods Zhang et al. employed watersheds as a feature representation and combined textural characteristics with anatomically structural characteristics to obtain precise liver segmentation. SVM, Neural Networks (NNs), Genetic algorithm, Deep Learning Machine, and other classifiers were employed to segment the liver. SVM is well designed for liver segmentation because it requires little additional training data. The ability of neural networks to describe nonlinear complicated associations among efforts and productions, as well as to discover designs in the statistics, make them ideal for liver separation. Furthermore, various machine learning algorithms have their own advantages, and as technology advances, more texture-based techniques will be used in image subdivision.

Tumor segmentation from the liver is the process of segregating liver cells from tumor cells. It is very important to segment tumor for any surgical operation. Accurate and precise location and shape of a tumor are a necessity for better treatment plan at different liver cancer stages.

This allows keeping track of the therapy over time. Various semi/automatic methods have been planned for liver cancer breakdown based on Bayesian approaches, entropy-based segmentations, level set techniques, multi-level thresholds, region growing techniques, SSMs, ML classifiers, graph cut, clustering, etc.

Pescia et al. used advanced nonlinear machine learning to figure out optimal features [69]. These optimal features were used by hyperplane to separate tumorous cells from non-tumorous cells in a liver tissue. Hong et al. proposed automatic system for perform liver tumor detection based on shape information and Fuzzy C-means clustering technique [70]. Statistical texture transforms (Haralick transforms) were used to calculate texture feature of an image by Koss et al. [70]. These features were then trained on Hopfield neural network to cluster into different organs. The method was tested using only one image and performance of the method was very low. A new liver image segmentation algorithm combining fuzzy C-means and multilayer perceptron neural network was proposed by Yuan et al. [71]. Luo et al. proposed pixel level texture feature extraction using wavelet transform which was feed into an SVM classifier for binary classification to determine liver and non-liver area [62]. This method had a misclassification error for both liver and non-liver pixel that required a set of morphological operation to get an accurate delineation of liver.

Freshly, there have been limited requests of a fully connected system to segment liver and liver tumor [72–74]. SVM and propagational learning were combined for tumor segmentation in the work of Zhou et al. citezhou2008semi. The SVM was learned on aimlessly particular samples in a ROI from a 2-D CT slice to extract tumor delineation of primary portion. This was followed by morphological operation of dilation and erosion projected in neighborhood slice for prediction of a tumor and was used recursively in adjacent slices. The SVM was qualified and efficient finished propagational erudition. Wong et al. established extra technique in which the feature was generated from a selected seed point [75]. 2D district increasing method was charity for segmenting tumor in liver. They also took some knowledge-based constraints into consideration to make sure that the shape and size of the segmented tumors are acceptable. In the work of Chen et al., a Detect Before Extract System was proposed to automatically find the liver boundary [76]. A specially designed feature descriptor was used to train a neural network classifier to differentiate between liver and two kinds of tumor: hepatoma and hemangioma. In their work, they classified two kinds of a liver tumor into 16 by 16 blocks instead of using texture feature to locate and segment tumor. Huang et al. proposed a new technique consuming kernel-based Extreme Learning Machine ELM) to notice and section liver tumor voxels in CT scans [77]. For training and testing, they have used feature vector associated with each voxel consisting of unkind and adjustment, entropy, law’s structures and summation and alteration histogram. The user was required to select tumor and non-tumor examples at the start to learn ELM classifier for voxel classification. Finally, morphological smoothing was used as a post-processing step to refine the segmented region of the tumor.

Chapter: 3

Methodology

3.1 Introduction

In this chapter, the SVM is utilised as a classifier for the segmentation of liver and tumour. SVM is another classifier for discrimination officially defined by hyperplane separation. Cortes and Vapnik first established the idea of SVM in 1995. The use of a hyperplane enables SVM to prevent the difficulty because of a variety of local minima in a smaller dimensions plane. In our thesis, we address the segmentation of the liver and tumour as a binary problem. We employed the SVM classificator in every segment during liver or lesion to determine whether or not the point is a liver or tumour cell. The separation between two cell kinds, i.e. liver or nonliver (for the segments of the liver) and tumour or non-tumor (for the segmentation of the tumour) was calculated with the aid of optimum Hyperplane SVM. The details of each algorithm and its implementation of the problem of liver and tumour segmentation are explained in the following sections.

3.2 Introduction and Construction of SVM Classifier

Vector support machines (SVMs) are machine learning techniques that may be used to classify, regress and discover outliers. The basic SVM concept can be viewed as nonlinear input vectors for mapping into higher dimensional areas and optimising separation planes for mapped vectors in space[104, 110]. [104, 110]. The SVM model trains from the example as space points to identify the large, unambiguous divide between point categories. Whenever a new example comes in, it may be mapped into the same larger area and forecasted into one category, depending about which side of the separating gap the points are falling.

The aforesaid optimal hyperplane is indeed the linear decision function (surface), with the maximum margin of two vectors of both classes, as seen in figure 4-2,. These hyperplanes can be built using relatively tiny quantities of training data, known as support vectors [111]. Below is the fundamental strategy for constructing the SVM hyperplane for input training sets.

3.3 PROPOSED LIVER TUMOR DETECTION ALGORITHM

Figure 1 shows the block illustration of the projected liver tumour division and discovery method. The method uses a pre-processing stage, function removal and arrangement with supporting vector machines.

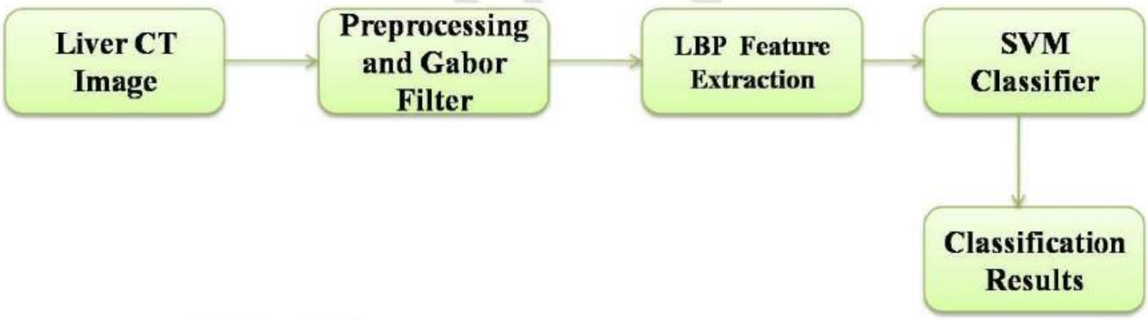

Preprocessing Image: Liver CT pictures are affected by noise throughout duplicate communication and digitalization during image processing. Pre-processing is a procedure through which these sounds are removed from the liver CT image. The contrast between the image and the liver with the surrounding soft tissues with the same intensity is improved in pre-processing step. Noise removal and contrast improvement are done with a medium filter and the image's fine features are further enhanced.

The Otsu Thresholding method is used in mathematical morphology median filtering. The Otsu algorithm uses the cumulative moments of the gray-level histogram 0th - and 1st -order. It is shown as,

$P = (ni)$, $P \geq 0$, $\sum L$ $P = 1$ (1)

i N i i–1

To identify the optimum inception value, it is essential to maximise the separation in grey levels between the resulting classes. Otsu's thresholding approach depends on whether the lowest point is selected amongst two grey level classes. The best threshold value k* can therefore be determined as follows:

a2(k∗) = max a2(k) (2)

1SkSL B

and the value of k is partial to:

$S* = \{k; mmO = m(k)[1 - m(k)] > 0, \quad \text{or} \quad 0 \le m(k) \le 1\}$ (3)

Morphological operations are utilised to advance increase the subdivision exactness of the tumour region. Morphological filters are employed to extract components of the image from the binary image in order to remove the area form, i.e. edges. The two activities in morphological processes are morphological initial and shutting.

Morphological Opening and Closing: A few morphological processes apply to the transformed binary image after converting the image to binary. The morphologic surgeon's principle is to separate the tumour portion of the image. The section of the tumour has the highest concentration than other imaging regions.

Both fundamental procedures, dilatation and erosion, are also coupled into more difficult sequences, namely opening and closure. Opening comprises of an erosion accompanied by a dilation and is used to remove pixels from areas too tiny to contain the structural element. Morphological opening alone is exploited in the suggested work.

Morphological opening is given by,

$A \circ B = (A \ominus B) \oplus B$ (4)

Gabor Transform: All pictures taken by a captured stratagem are in three-dimensional sphere style (Amplitude vs Time). The Fourier transform (FT) is used to transform the province method to occurrence (Single Resolution Mode–Freq vs amplitude). In Multi Resolution mode, i.e., frequency vs. time, we require the Liver CT image. We utilise Gabor Wavelet, hence.

Gabor Transform: All pictures taken by a captured trick are in longitudinal domain mode (Time vs. Amplitude). The Fourier transform (FT) is used to transform the domain mode to frequency (Single Resolution Mode–Freq vs amplitude). In Multi Resolution mode, i.e., frequency vs. time, we require the Liver CT image. We utilise Gabor Wavelet, hence.

k2 k2 z2 a2

f = μ, v exp (− μ, v) × [exp (ik z) – exp (−)] (5) _μ, v a2 2a2 μ, v2

Where the Gabor kernels orientation and scale are μ & μ, the wave vector is z=(x,y) and kμ,v. Extraction feature:

Binary Local Pattern Features: The Efficient Texture Based Operator is Local Binary Pattern (LBP). It operates by labelling the image pixels by threshing each pixel neighbourhood and saves the output as a binary number. The LBP operator has a simple computation; hence the liver CT images can be analysed in real-time uses.

LBP over spatial domain: the LBP operator creates a two-dimensional surface structure with two additional measurements, that is, grey difference and local longitudinal designs. For pixels in the image, the LBP operator produces labels that threshold the surrounding 3/3 pixels with the central value and saves the consequence as a binary integer. In unchecked design separation, the LBP operator can be utilised to generate higher performance in tandem with the local contrast measure.

The image is covered with a 3x3 mask window and a sub-image is gotten. In the ensuing 3x3 sub-image, the centre pixel value is compared to its nearest pixels. If the nearest pixel is more than the pixel centre, the next pixel value will be swapped by 1, or the next pixel value will be swapped by 0. Finally, all of the nearby pixels are changed by either 0 or 1, when a binary number of eight digits is merged. Figure 2 explains the detailed operation.

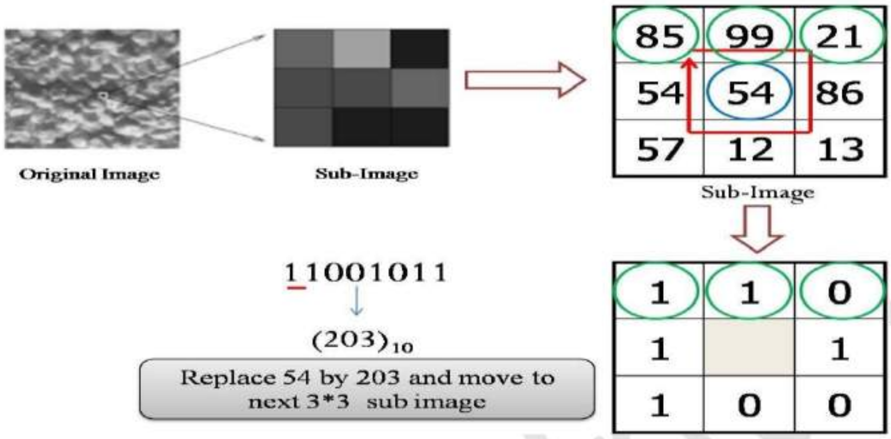

SVM Arrangement: Support Vector Machine (SVM) is a linear, self-learning classifier that is high efficiency, the most accurate classifier. Vapnik introduced SVMs in 1998. Although the SVM classification method wants a very long duration of exercise, it is dimensional and also independent of space. SVM is a feed-in network with a single non-linear unit layer, with very accurate classification results of SVM.

SVM operates on the premise of reducing the binding of errors generated during training by the learning appliance on the test dataset. The goal purpose of the exercise datasets is not minimised. Thus, by concentrating on and learning tough data sets throughout its training process, SVM can operate effortlessly over imageries which do not correspond to exercise data sets. Data sets in training are termed support vectors, which are very tough to classify.

In simple, SVM finds the hyperplane in which decision functions are largely separated into two classes even for challenging datasets. Figure 3 shows both classes separated by a margin labelled 'X' and 'O' following the hyper-plane position using SVM sorting. The support vectors are existing near the hyperplane border of the two curriculums.

If a projection $0: X \square H$ is used, the dot product is represented by a kernel function k,

$$k(x, x') = \langle 0(x), 0(x') \rangle \qquad (6)$$

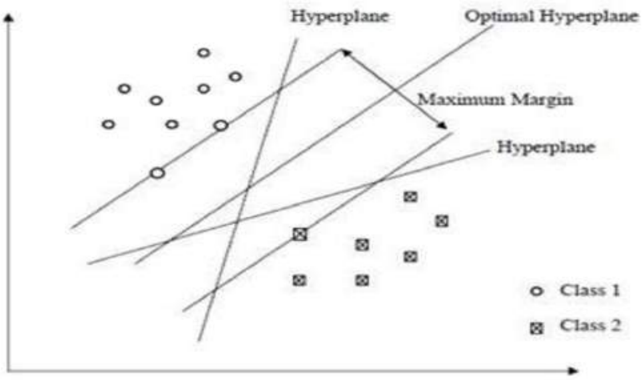

Fig. 3 SVM classification method

By reviewing different factors related to the research it is derived that the research methodologies is based on enhanced, correlated, modified and particularly focused on various aspects and factors of research paradigm. The theoretical knowledge of the research reflects that our research is based on secondary research by unrevealing different features and gets the desired objectives by emphasizing on previous theoretical concepts. By jumping towards the practically implementations of the research the theoretical methodologies are molded in such a way where quantitative and analyzing images of patient's datasets are in used and collected from different hospitals which is based on liver cancer prediction and detection purpose. Sudhamani et al. (2014) also adopted the similar approach to test 100 CT images of 63 patients by using MATLAB. Hence by using enhanced algorithm better accuracy is obtained and through images datasets detection and prediction phenomena is succeeded. It happens to be only reliable approach that achieves efficient accuracy and better prediction and detection results. Ali et al. (2014) study is also more or less based on the same concept.

Chapter: 04

Results and Analysis

4.1 Liver cancer presentation

The presentation of liver cancer breakdown is investigated with the succeeding limitations:

• Sensitivity [Se=TP / (TP+FN)]

• Specificity [Sp=TN / (TN+FP)]

• Positive predictive value [Ppv=TP/(TP+FP)]

• Negative predictive value [Npv=TN/(TN+FN)]

• Accuracy [Acc=(TP+TN)/(TP+FN+TN+FP)]

These limitations. TP is true positive, FP is false positive, FN is false negative and TN is true negative. True Positive raises to the proper tumour pixels, True Negative refers to incorrectly identified tumour pixels, and False Positive refers to properly detected pixels, and False Negative refers to incorrectly recognized pixels for the tumour.

Limitations Se and Sp describe the ratio of well-classified tumour pixels to non-tumor pixels. Ppv is the ratio of pixels categorised as correctly classified tissue pixels. Npv is the fraction of pixels which are rightly categorised as background pixels. Finally, Acc is a ratio of total tumour pixels that are well detected and categorised. The performance of our suggested classification algorithm is defined by all these criteria.

The diagnosis of liver tumours is an important medical criterion. In this work, the tumour region is detected and segmented in the liver CT picture. A vector support machine is used to diagnose the segmented liver tumour, which subsequently classifies the liver tumour as benign or malignant. Sensitivity, specificities, optimistic prognostic value, adverse predictive value and accuracy are then analysed. The average accuracy obtained for malignant tumour regions is 95 percent in line with photographs of ground truth. The dataset used in this experiment is shown in Fig. 1. The data comprises gentle and hateful tumour photos of the liver.

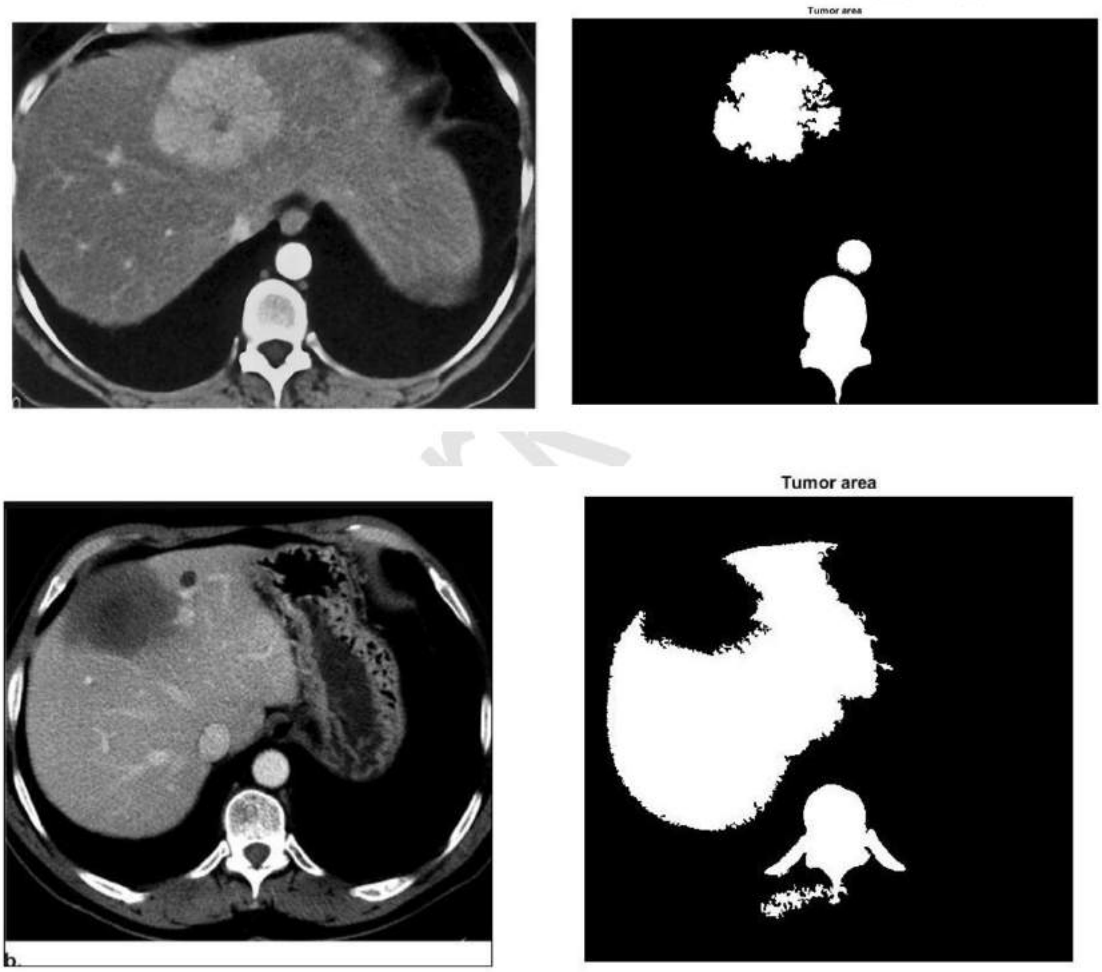

Fig. 1 (a)-(b) liver test image

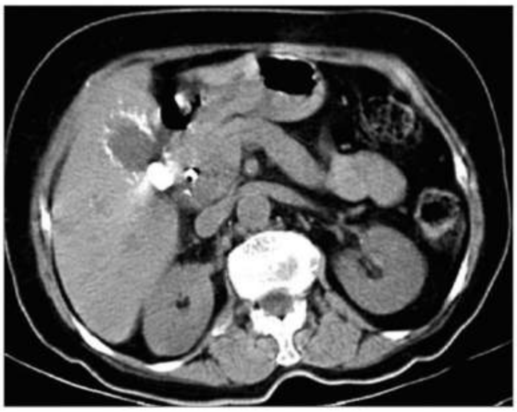

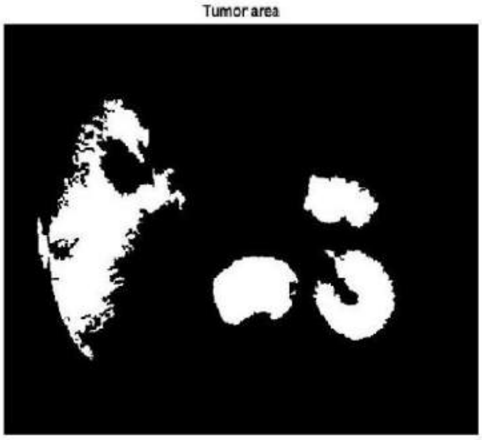
Tumor area

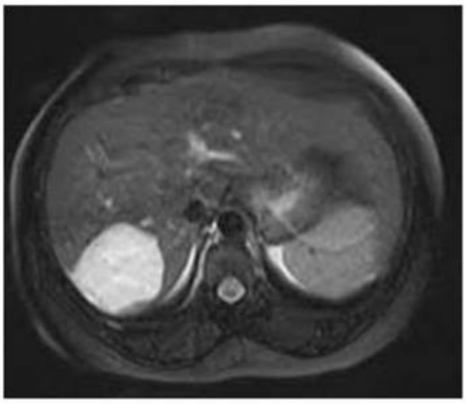

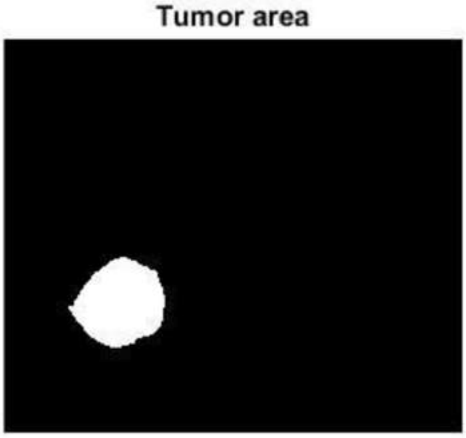
Tumor area

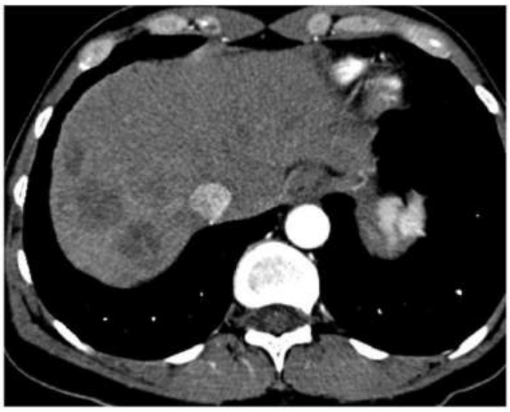

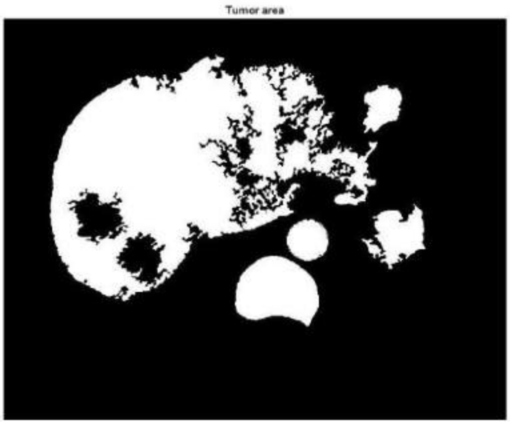
Tumor area

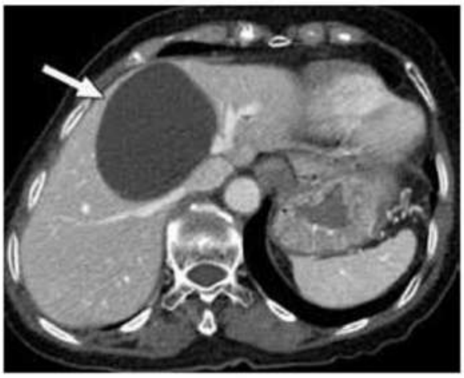

Tumor area

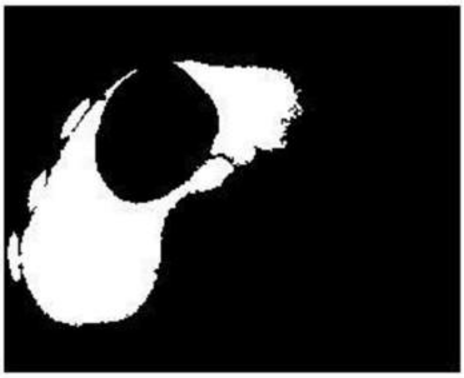

Tumor area

Tumor area

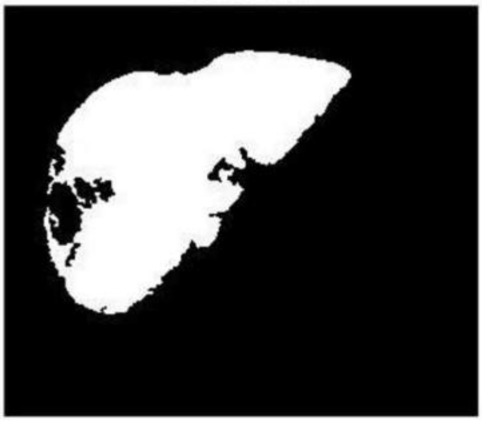

Tumor area

Tumor area

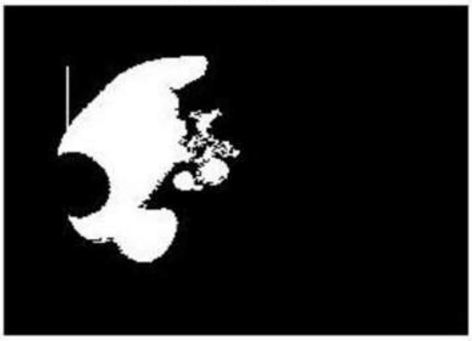

Tumor area

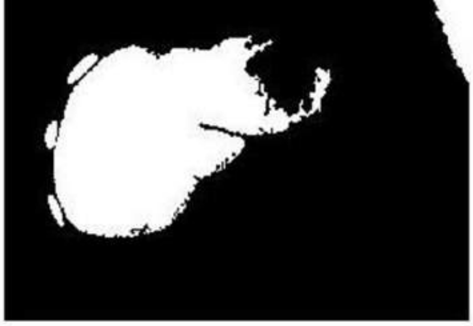

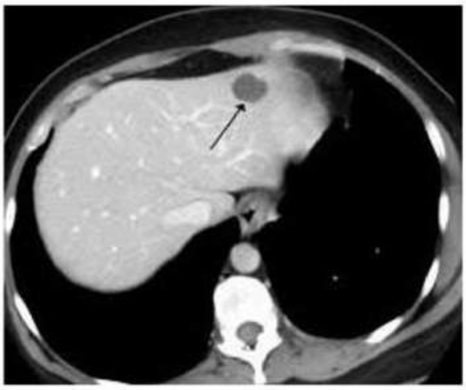

Tumor area

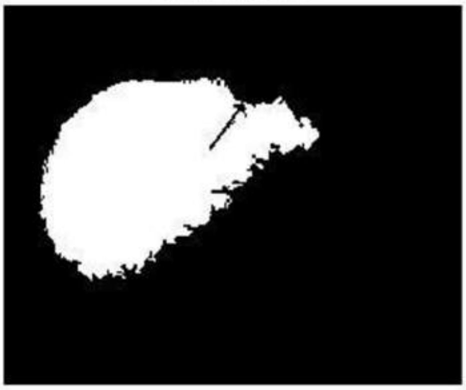

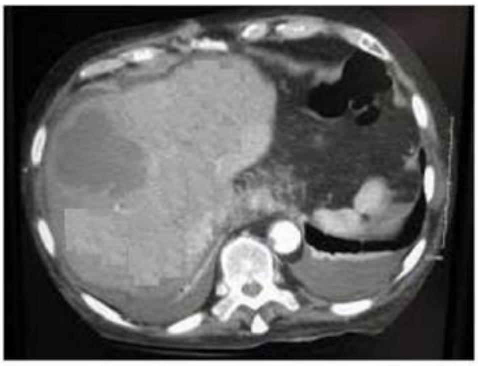

Tumor area

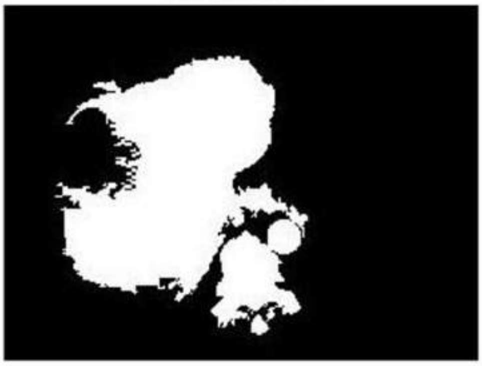

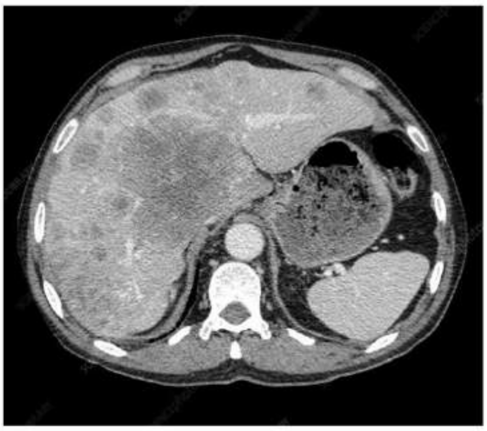

Tumor area

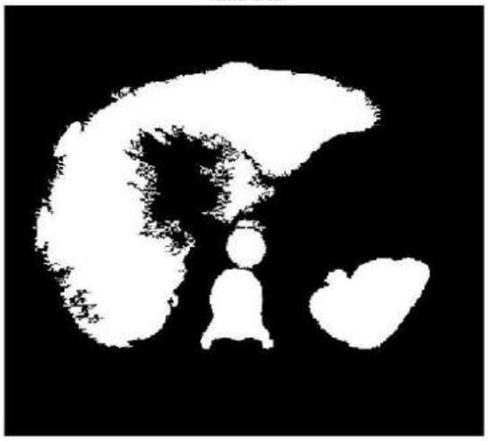

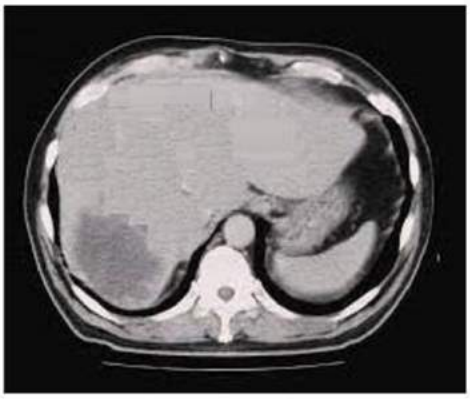

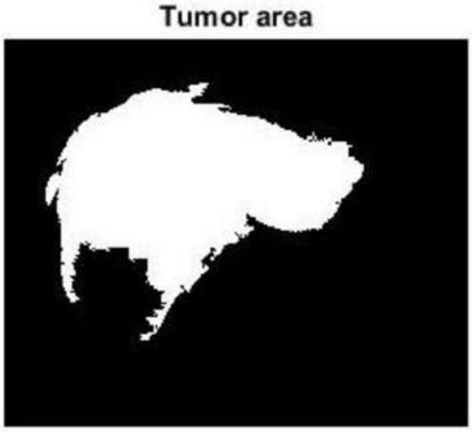
Tumor area

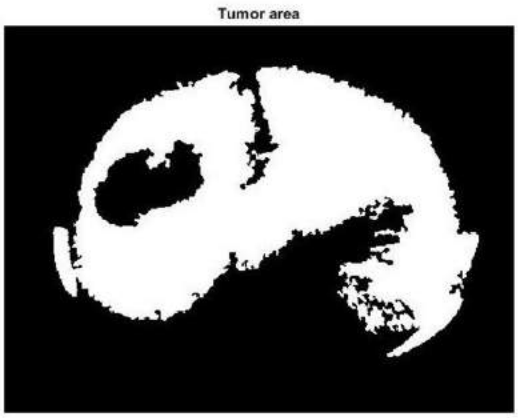
Tumor area

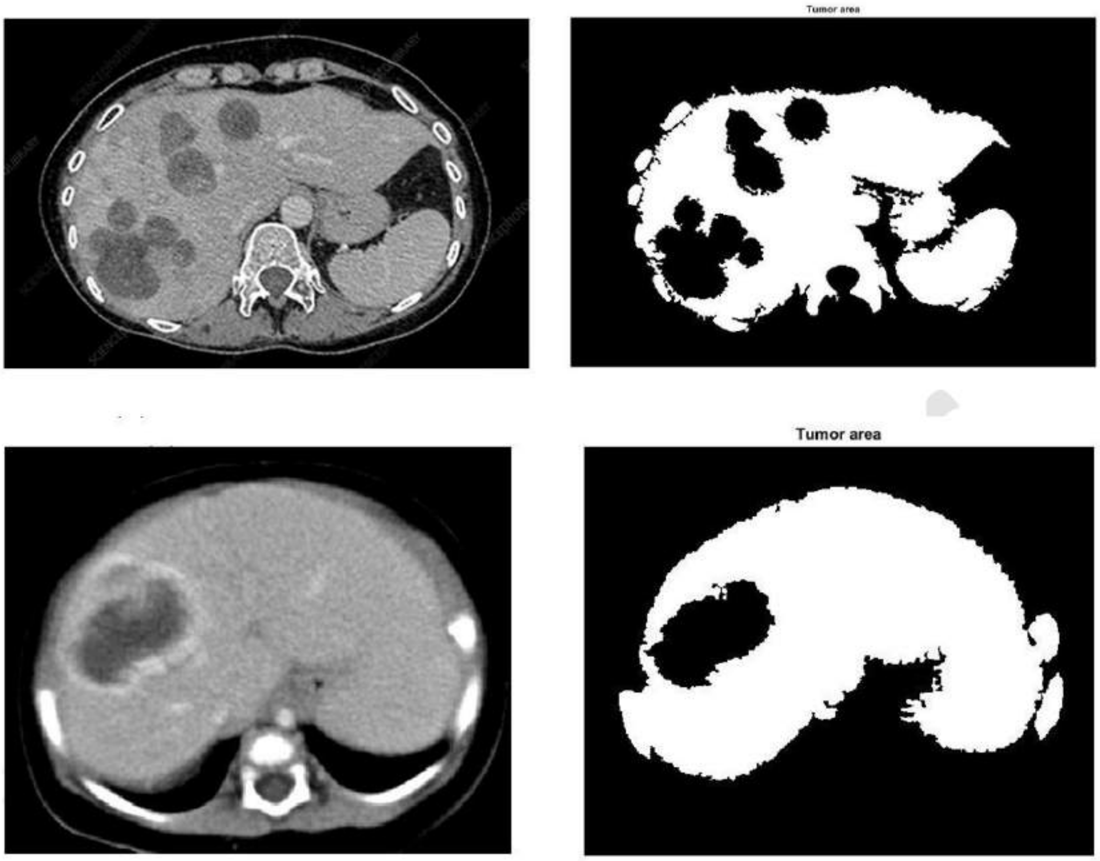

4.2 Confusion Matrix

Confusion matrix describes the classifiers performance based on the training and validation data. It represents a comparative analysis of true positive and true negatives. Moreover, measurements of the accuracy, sensitivity, specificity and precision are also evident from the confusion matrix. It describes how much cases are truly or falsely diagnosed by the system. 4 possible outcomes are there: -

- **True Positive (TP):** A true positive outcome describes the correct prediction of the positive class. For example, if a patient has coronavirus disease and it is correctly identified from the symptoms by the expert system is counted as true positive score of the system. In medical diagnostic terms, it is also called sensitivity of the testing algorithm.

- **False Positive (FP)**: A false positive outcome describes the scenario in which system identified a patient as a covid-19 disease by reading his symptoms file while the patient has no heart at all. This is also known as wrong prediction as the positive class. In medical diagnostic terms, it is also called specificity of the test.
- **True Negative (TN)**: A true negative outcome describes the correct prediction of the negative class. For example, if a patient doesn't have covid-19 disease and it is correctly identified from the symptoms by the expert system is counted as true negative score of the system.
- **False Negative (FN)**: A false negative outcome describes the scenario in which system identified a patient as "no disease indication" by reading his symptoms file while the patient has coronavirus disease.

According to the confusion matrix, our model has correctly diagnosed 249 instances out of 271 instances. And in case of no disease instance, it correctly classified 237 out of 281 instances. These performance statistics, recall/sensitivity, precision and algorithm performances is produced by the expert system and reflected in the form of Confusion Matrices. Tables No. 4.2, given as under show the Confusion Matrices for proposed Expert System based on CNN.

Fusion Based CNN

N=550		**Predicted**	
		Yes	**No**
Actual		$True_{Positive}$	$False_{Positive}$
	Yes	249	22
	No	$False_{Negative}$	$True_{Negative}$

		44	237

Table 4. 1 Confusion Matrix of Proposed Model

Tables No. 4.3, given as under show the Confusion Matrices for detection of covid using Inception Model from X-rays.

Inception Model using X-rays

N=402		Predicted	
		Yes	No
Actual	Yes	$True_{Positive}$ 201	$False_{Positive}$ 0
	No	$False_{Negative}$ 13	$True_{Negative}$ 188

Table 4. 2 Confusion Matrix of InceptionV3 (CXR)

Tables No. 4.4, given as under show the Confusion Matrices for detection of covid using Inception Model from CT scans.

Inception Model using CT scans

N=150		Predicted	
		Yes	No
Actual	Yes	$True_{Positive}$ 44	$False_{Positive}$ 26
	No	$False_{Negative}$ 10	$True_{Negative}$ 70

Table 4. 3 Fusion Matrix of InceptionV3 (CT scan)

Table 4. 4

Tables No. 4.5, given as under show the Confusion Matrices for detection of covid using VGG-16 Model from CT scans.

VGG-16 using CT scans

N=150		Predicted	
		Yes	No
	Yes	$True_{Positive}$	$False_{Positive}$

Actual		48	22
	No	$False_{Negative}$ 31	$True_{Negative}$ 49

Table 4. 4 Confusion Matrix of VGG-16 (CT scan)

Tables No. 4.6, given as under show the Confusion Matrices for detection of covid using VGG-16 Model from X-rays.

VGG-16 using X-rays

N=402		**Predicted**	
		Yes	**No**
Actual	**Yes**	$True_{Positive}$ 186	$False_{Positive}$ 15
	No	$False_{Negative}$ 124	$True_{Negative}$ 77

Table 4. 5 Confusion Matrix of VGG-16 (CXR)

From the given confusion matrix, it is clearly defined that inceptionv3 model prediction is move accurate on x-rays images as compared to VGG-16 model on x-rays. And also indicate that VGG-16 model predict more accurate on CT scan as compared to InceptionV3 model. For this we can conclude the use of inceptionV3 pretrained model for extracting features from x-rays is best and VGG-16 model is best for extracting features from CT scans.

Accuracy can be defined as under:-

$$\textbf{Accuracy} = \frac{True_{Positive} + True_{Negative}}{True_{Positive} + True_{Negative} + False_{Positive} + False_{Negative}} \qquad \text{Eq. 4.1}$$

Sensitivity or Recall can be calculated through the following equation:-

$$\textbf{Sensitivity} = \frac{True_{Positive}}{True_{Positive} + False_{Negative}} \qquad \text{Eq. 4.2}$$

Calculation of specificity:-

$$\textbf{Specificity} = \frac{True_{Negative}}{True_{Negative} + False_{Positive}} \qquad \text{Eq. 4.3}$$

Calculation of precision:-

$$\textbf{Precision} = \frac{True_{Positive}}{True_{Positive} + False_{Positive}} \qquad \text{Eq. 4.4}$$

Equation 4.5 shows negative predictive rate

$$\textbf{Negative Predictive Rate} = \frac{True_{Negative}}{True_{Negative} + False_{Negative}} \qquad \text{Eq. 4.5}$$

Equation 4.6 shows false positive rate

$$\textbf{False Positive Rate} = \frac{False_{Positive}}{True_{Negative} + False_{Positive}} \qquad \text{Eq. 4.6}$$

Equation 4.7 shows false negative rate

$$\textbf{False Negative Rate} = \frac{False_{Negative}}{False_{Negative} + True_{Positive}} \qquad \text{Eq. 4.7}$$

Chapter: 05

Conclusion

We proposed a new method and validation research in which the liver tumours of the liver CT picture are automatically segmented. The segmentation method suggested in this study provides a new method for classifying tumours that assists medical experts to diagnose further. Our key benefit is that it provides precise findings for many forms of liver cancers easily and without manual intervention.

The proposed liver lesion characterization framework's competitive performance is related to its robust underlying structure, aimed to better characterise hepatic lesions using numerous ROIs and previous medical knowledge. Further, the analogy between the radiological findings and the use of the links among low-level and high-level properties in the selection of ROIs are the keys to its efficient lesion capture.

In contrast to the majority of baselines, lesions are characterised by identical cases or lesions of their self without paying regard to the association among scratch and hepatitis.In calculation, the benefit of the suggested agenda to boost the presentation of the lesion categorization with an interpretable characterization that supports the diagnostic choice. Unlike most current investigation, which solely uses low-level black box structures.

Two datasets conducted a complete set of measurement metrics (Dataset I and overall dataset). This was done to examine the inclusive performance and classification agenda of lesion characterization. A comparative assessment of characterization and classification accuracy and benchmarking with the latest hard set of connected works are offered. The investigational consequences and the inclusive benchmarking of the particular baselines showed the suggested framework capacity to identify and classify liver lesions with greater precisions.

Moreover, the arithmetical examination indicated that the findings of the approach projected are highly statistically noteworthy associated to other present ways for the classification of liver lesions, with interpretable characterization benefiting.

The thesis stated, however, that the suggested framework for lesion characterization has several advantages; the first is the characterization of hepatitis lesion with high precision and the increased number of high-level characteristics than the rest of the researchers.

The second advantage is the capacity to highly accurately categorize the liver lesion, with the benefit of an interpretation of the choice in human underestimation and equivalent to the surveillance by the radiologist. The third benefit is its generosity, which makes the data sets with diverse CT image settings and resolution applicable. The technique suggested can be further enhanced in the future employing neural networks and fuzzy algorithms.

Reference

American Cancer Society, liver cancer [online], Available: www.cancer .org accessed: [22-01-2016].

American national society, history of cancer, [online], Available: www.m.cancer.com Accessed: [10-02-2016].

American Society of Clinical Oncology. [Online], Available: www.cancerprogress.net/timeline/major-milestones-against-cancer accessed: [10-02, 2016]

Ananthakrishnan Ashwin, Veena Gogineni, and Kia Saeian, (2006). Epidemiology of primary and secondary liver cancers. Seminars in interventional radiology, 23(1), 43-47.

Assaf Hoogi, Arjun Subramaniam et al, (2016). Adaptive estimation of active contour parameters using convolutional neural networks and texture analysis. IEEE Transactions on Medical Imaging,36 (3), 781-791.

Belgherbi, A., Hadjidj, I., Bessaid, A, “Semi-automated Method for the Liver Lesion Extraction from a CT Images Based on Mathematical Morphology”, iMedPub Journals Journal Of Biomedical Sciences, Vol. 2 No. 2:4, doi: 10.3823/1019, PP 1-9, 2013

Bosch, F. Xavier, Josepa Ribes, Mireia Díaz, and Ramon Cléries, (2004). Primary liver cancer: worldwide incidence and trends. Gastroenterology, 127(5), S5-S16.

Boykov YY, Jolly MP (2001) Interactive graph-cuts for optimal boundary and region segmentation of objects in N-D images. ICCV, Vancouver, 1, 105-112

Christ PF, Elshaer MEA, Ettlinger F et al., (2016). Automatic liver and lesion segmentation in CT using cascaded fully convolutional neural networks and 3D conditional random fields. MICCAI 2016, 19th International Conference on Medical Image Computing and Computer Assisted Intervention, Athens, 9901, DOI: 10.1007/978-3- 319-46723-8-48.415-423

Dr. S. Vijayarani, Mr.S.Dhayanand, “Liver Disease Prediction using SVM and Naïve Bayes Algorithms”, International Journal of Science, Engineering and Technology Research (IJSETR), ISSN: 2278 – 7798, Volume 4, Issue 4, PP 816-820, April 2015.

E-Liang Chen, Pau-Choo Chung, Hong-Ming Tsai, and Chein-I Chang, "An Automatic Diagnostic System for CT Liver Image Classification", IEEE Transactions On Biomedical Engineering, Vol. 45, No. 6, June 1998, PP 783-794.

Gabriel Chartrand, Thierry Cresson et al, (2016). Liver Segmentation on CT and MR Using Laplacian Mesh Optimization. IEEE Transactions on Biomedical Engineering, 64(9), 2110-2121

Guodong Li , Xinjian Chen, Fei Shi, Weifang Zhu, Jie Tian, (2015). Automatic Liver Segmentation based on Shape Constraints and Deformable Graph Cut in CT Images. IEEE Transactions on Image Processing, 24(12), 5315-5329.

Guohui Zhou, Yuanyuan Wang, Weiqi Wang, "Diagnosis of Hepatic Fibrosis by Ultrasonic Image Analysis", IEEE International Conference on Biomedical Engineering and Biotechnology, DOI 10.1109 978-0-7695-4706-0/12, Dec 2012, PP 775-776.

Hu, Z., Tang, J., Wang, Z., Zhang, K., Zhang, L. & Sun, Q. (2018). Deep learning for image based cancer detection and diagnosis-A survey. Pattern Recognition, 83,134-149.

Huang, Y., Chen, J. & Shen, W. (2004). Computer-aided diagnosis of liver tumors in non-enhanced CT images. Journal Medical Physics, 9,141–50.

Huang, Y., Chen, J. & Shen, W. (2004). Computer-aided diagnosis of liver tumors in non-enhanced CT images. Journal Medical Physics, 9,141–50.

Hussein Alahmer, Amr Ahmed, "Computer-Aided Classification of Liver Lesions Using Contrasting Features Difference" white paper.

Ji, Z., & Wang, B. (2014). Identifying potential clinical syndromes of hepatocellular carcinoma using PSO-based hierarchical feature selection algorithm. Biomed research international Conference, DOI: 10.1155/2014/127572, 1-12.

Jiang, H., Zheng, R., Yi, D. & Zhao, D. (2013). A novel multi-instance learning approach for liver cancer recognition on abdominal CT images based on CPSO-SVM and IO. Computational and Mathematical Methods Medicine, 2013, 1-10

Jie L, Defeng W, Lin S, Pheng A. H., (2012). Automatic liver segmentation in CT images based on support vector machine. EEE-EMBS International Conference on Biomedical and Health Informatics, 2012, 33-336

Joshi, Narendra D Londhe, "Automatic Liver Tumour Detection in Abdominal CT Images", International Journal of Computer Technology and Electronics Engineering (IJCTEE), Volume 3, Issue 1, PP 25-30 February 2013.

Kaijian XIA, Hongsheng YIN et al., (2017). Liver Semantic Segmentation Algorithm Based on Improved Deep Adversarial Networks in combination of Weighted Loss Function on Abdominal CT Images. IEEE Access, 7, 96349-96358.

Li, C., Wang, X., Fulham, S.E.M., Yin, Y., Chen, J. & Feng, D.D. (2013). A likelihood and local constraint level set model for liver tumor segmentation from CT volumes. IEEE Transactions on Biomedical Engineering, 60(10), 2967-2977.

Lopez-Mir F, Gonzalez P, Naranjo V, Pareja E, Alcaniz M, SolazMinguez J (2013). A fast computational method based on 3D morphology and a statistical filter. International Conference on Bioinformatics and Biomedical Engineering, 483–490. .

Lu, F., Wu, F., Hu, P., Peng, Z. & Kong, D. (2017). Automatic 3D liver location and segmentation via convolutional neural network and graph cut. International Journal of computer Assisted Radiology and Surgery, 12, 171-182.

Megha P Arakeria and G Ram Mohana Reddy, "Recent Trends and Challenges in CAD of Liver Cancer onCT Images", International Journal of Information Processing, 6(1), 50-59, ISSN : 0973-8215 IK International Publishing House Pvt. Ltd., New Delhi, India, PP 50-50, 2012.

Norajitra T, Meinzer H. P., Maier-Hein K. H., (2015). 3D statistical shape models incorporating 3D random forest regression voting for robust CT liver segmentation. Medical Imaging 2015: Computer-Aided Diagnosis. SPIE, Orlando, 941406, 1-6.

P. Campadelli, E. Casiraghi and A. Esposito, (2009). Liver Segmentation from Computed Tomography Scans: A Survey and a New Algorithm. Artificial Intelligence in Medicine, 45(3), 185-196

Qin Zhang, Yingfang Fan et al., (2017). An Efficient and Clinical-Oriented 3D Liver Segmentation Method. IEEE Access, 5, 18737-18744

R.Rajagopal, P.Subbiah, "Computer Aided Detection of Liver Tumor using SVM Classifier", International Journal of Advanced Research in Electrical, Electronics and

Instrumentation Engineering, ISSN (Print) : 2320 – 3765, ISSN (Online): 2278 – 8875, Vol. 3, Issue 6, PP 10170-10177, June 2014.

Ramandeep Kaur Bhullar, Navpreet Kaur Walia,, "A New Hybrid Technique for Detection of Liver Cancer on Ultrasound Images" International Journal of Science and Research (IJSR), ISSN (Online): 2319-7064, Impact Factor (2012): 3.358, Volume 3 Issue 10, PP 1647-1651, October 2014.

S. Priyadarsini and D. Selvathi, (2012). Survey on Segmentation of Liver from CT Images. 2012 IEEE International Conference on Advanced Communication Control and Computing Technologies, 2012, 25-32.

Sharma N, Aggarwal LM (2010). Automated medical image segmentation techniques. Journal of Medical Physics, 35(1), 3-14

Sun, C., Guo, S., Zhang, H., Li, J., Chen, M., Ma, S., Jin, L., Liu, X., Li, X. & Qian, X. (2017). Automatic segmentation of liver tumors from multiphase contrast-enhanced CT images based on FCNs. Artificial Intelligence in Medicine, 83, 58-66

V. Ulagamuthalvi, D. Sridharan, "Liver Cancer Tumor Segmentation on ultrasound images", International Journal of Computational Intelligence and Informatics, Vol. 2: No. 1, PP 68- 71, April - June 2012.

Song, Y.; Cai, W.; Zhou, Y.; Feng, D.D. Feature-Based Image Patch Approximation for Lung Tissue Classification. IEEE Trans. Med Imaging 2013, 32, 797–808.

Nugroho, H.A.; Frannita, E.L.; Ardiyanto, I.; Choridah, L. Computer aided diagnosis for thyroid cancer system based on internal and external characteristics. J. King Saud Univ. Comput. Inf. Sci. 2019.

Chen, Y.; Yue, X.; Fujita, H.; Fu, S. Three-way decision support for diagnosis on focal liver lesions. Knowl.-Based Syst. 2017, 127, 85–99.

Kumar, S.; Moni, R.; Rajeesh, J. An automatic computer-aided diagnosis system for liver tumours on computed tomography images. Comput. Electr. Eng. 2013, 39, 1516–1526.

Gunasundari, S.; Janakiraman, S.; Meenambal, S. Multiswarm heterogeneous binary PSO using win-win approach for improved feature selection in liver and kidney disease diagnosis. Comput. Med Imaging Graph. 2018, 70, 135–154.

Chang, C.-C.; Chen, H.-H.; Chang, Y.-C.; Yang, M.-Y.; Lo, C.-M.; Ko, W.-C.; Lee, Y.-F.; Liu, K.-L.; Chang, R.-F. Computer-aided diagnosis of liver tumors on computed tomography images. Comput. Methods Programs Biomed. 2017, 145, 45–51.

Bian, C.; Lee, R.; Chou, Y.-H.; Cheng, J.-Z. Boundary Regularized Convolutional Neural Network for Layer Parsing of Breast Anatomy in Automated Whole Breast Ultrasound. In Proceedings of the Medical Image Computing and Computer Assisted Intervention—MICCAI 2017, Quebec City, QC, Canada, 11–13 September 2017; pp. 259–266.

Xu, K.; Roussel, P.; Csapó, T.G.; Denby, B. Convolutional neural network-based automatic classification of midsagittal tongue gestural targets using B-mode ultrasound images. J. Acoust. Soc. Am. 2017, 141, EL531–EL537.

Xie, H.; Yang, D.; Sun, N.; Chen, Z.; Zhang, Y. Automated pulmonary nodule detection in CT images using deep convolutional neural networks. Pattern Recognit. 2019, 85, 109–119.

Chitradevi, D.; Prabha, S. Analysis of brain sub regions using optimization techniques and deep learning method in Alzheimer disease. Appl. Soft Comput. 2019, 86, 105857.

Beloufa, F.; Chikh, M. Design of fuzzy classifier for diabetes disease using Modified Artificial Bee Colony algorithm. Comput. Methods Programs Biomed. 2013, 112, 92–103.

Prasartvit, T.; Banharnsakun, A.; Kaewkamnerdpong, B.; Achalakul, T. Reducing bioinformatics data dimension with ABC-kNN. Neurocomputing 2013, 116, 367–381.

Lam, K. Y., Tsang, N. W. H., Han, S., and Zhang, W., Ng, J. K. Y., & Nath, A. (2017). Activity tracking and monitoring of patients with Alzheimer's disease. Multimedia Tools and Applications, 76(1), 489-521.

A. Norouzi, M.S.M. Rahim, A. Altameem, T. Saba, A.E. Rada, A. Rehman, et al.

Medical image segmentation methods, algorithms, and applications

Iete Tech Rev, 31 (3) (2014), pp. 199-213, 10.1080/02564602.2014.906861

L.R. Bareiro Paniagua, D.N. Leguizamón Correa, D.P. Pinto-Roa, J.L. Vázquez Noguera, S. Toledo, A. Lizza

Yip, T. F., Ma, A. J., Wong, V. S., Tse, Y. K., Chan, H. Y., Yuen, P. C., & Wong, G. H. (2017). Laboratory parameter-based machine learning model for excluding non-alcoholic fatty liver disease (NAFLD) in the general population. Alimentary Pharmacology & Therapeutics.

Ting-tingzhao1, yu-boyuan1, yingjiewang 2, jugao, ping¬he. (¬2017). Heart disease classificati on based on featur efusion, *oufsobujpobm$pogfsfodfpo.bdijoffbsojohboe$zcfsofujdt

Zhang, J., Gong, J., & Barnes, L. (2017, July). HCNN: Heterogeneous Convolutional Neural Networks for Comorbid Risk Prediction with Electronic Health Records. In Connected Health: Applications, Systems and Engineering Technologies (CHASE), 2017 IEEE/ACM International Conference on (pp. 214-221). IEEE.

Tripoliti, E. E., Papadopoulos, T. G., Karanasiou, G. S., Kalatzis, F. G., Bechlioulis, A., Goletsis, Y., & Fotiadis, D. I. (2017, February). Estimation of New York Heart Association class in heart failure patients based on machine learning techniques. In Biomedical & Health Informatics (BHI), 2017 IEEE EMBS International Conference on (pp. 421-424). IEEE.

Kim, E. Y., Lee, M. Y., Kim, S. H., Ha, K., Kim, K. P., & Ahn, Y. M. (2017). Diagnosis of major depressive disorder by combining multimodal information from heart rate dynamics and serum proteomics using machine-learning algorithm. Progress in Neuro-Psychopharmacology and Biological Psychiatry, 76, 65-71

Lee, S., Sugimoto, K., & Okada, Y. (2017, September). Detection of abnormal ECG waveform based on linkage pattern mining. In Biometrics and Kansei Engineering (ICBAKE), 2017 International Conference on (pp. 37-41). IEEE.

Dominguez-Morales, J. P., Jimenez-Fernandez, A. F., Dominguez Morales, M. J., & Jimenez-Moreno, G. (2017). Deep Neural Networks for the Recognition and Classification of Heart Murmurs Using Neuromorphic Auditory Sensors. IEEE transactions on biomedical circuits and systems

] Hongxu, Y. I. N., & Jha, N. (2017). A Hierarchical Health Decision Support System for Disease Diagnosis based on Wearable Medical Sensors and Machine Learning Ensembles. IEEE Transactions on Multi-Scale Computing Systems.

Timothy, V., Prihatmanto, A. S., & Rhee, K. H. (2016, December). Data preparation step for automated diagnosis based on HRV analysis and machine learning. In Frontiers of Information Technology (FIT), 2016 International Conference on (pp. 142-148). IEEE.

] Ekız, S., & Erdoğmuş, P. (2017, April). Comparative study of heart disease classification. In Electric Electronics, Computer Science, Biomedical Engineerings' Meeting (EBBT), 2017 (pp. 1-4). IEEE.

] _YU-BOYUAN1, WEN-QIANGQIU1, YINGJIEWANG2, JUGAO¬2, PINGHE3. (2017). CLASSIFICATION OF HEART FAILURE WITH POLYNOMIAL SMOOTH SUPPORT VECTOR MACHINE. 2017 IEEE

McRae, M. P., Bozkurt, B., Ballantyne, C. M., Sanchez, X., Christodoulides, N., Simmons, G., ... & Campbell, C. (2016). Cardiac ScoreCard: a diagnostic multivariate index assay system for predicting a spectrum of cardiovascular disease. Expert Systems with Applications, 54, 136-147.

Uçar, M. K., Bozkurt, M. R., Bilgin, C., & Polat, K. (2016). Automatic sleep staging in obstructive sleep apnea patients using photoplethysmography, heart rate variability signal and machine learning techniques. Neural Computing and Applications, 1-16.

Acharya, U. R., Fujita, H., Lih, O. S., Adam, M., Tan, J. H., & Chua, C. K. (2017). Automated Detection of Coronary Artery Disease Using Different Durations of ECG Segments with Convolutional Neural Network. Knowledge-Based Systems.

] Kumar, M., Pachori, R. B., & Acharya, U. R. (2016). An efficient automated technique for CAD diagnosis using flexible analytic wavelet transform and entropy features extracted from HRV signals. Expert Systems with Applications, 63, 165-172.

Gagnon, L. L., Gagnon-Turcotte, G., Popek, A., Chatelier, A., Chahine, M., & Gosselin, B. (2017, May). A wireless system for combined heart optogenetics and electrocardiography recording. In Circuits and Systems (ISCAS), 2017 IEEE International Symposium on (pp. 1-4). IEEE

] Luo, Y., Yang, B., Xu, L., Hao, L., Liu, J., Yao, Y., & van de Vosse, F. (2017). Segmentation of the left ventricle in cardiac MRI using a hierarchical extreme learning machine model. International Journal of Machine Learning and Cybernetics, 1-11.

] Alić, B., Gurbeta, L., & Badnjević, A. (2017, June). Machine learning techniques for classification of diabetes and cardiovascular diseases. In Embedded Computing (MECO), 2017 6th Mediterranean Conference on (pp. 1-4). IEEE.

K. Vaishnavee, K. Amshakala

An automated MRI brain image segmentation and tumor detection using SOM-clustering and proximal support vector machine classifier

2015 IEEE International Conference on Engineering and Technology (ICETECH), IEEE (2015), pp. 1-6

CrossRefView Record in ScopusGoogle Scholar

M. Arikan, B. Fröhler, T. Möller

Semi-automatic brain tumor segmentation using support vector machines and interactive seed selection Proceedings MICCAI-BRATS Workshop (2016), pp. 1-3 View Record in ScopusGoogle Scholar

A. Ellwaa, A. Hussein, E. Alnaggar, M. Zidan, M. Zaki, M.A. Ismail, et al. Brain tumor segmantation using random forest trained on iteratively selected patients International Workshop on Brainlesion: Glioma, Multiple Sclerosis, Stroke and Traumatic Brain Injuries (2016), pp. 129-137 CrossRefView Record in ScopusGoogle Scholar S. Abbasi, F. Tajeripour

Detection of brain tumor in 3D MRI images using local binary patterns and histogram orientation gradient Neurocomputing, 219 (2017), pp. 526-535 ArticleDownload PDFView Record in ScopusGoogle Scholar

Mehmood, M. Sajjad, K. Muhammad, S.I.A. Shah, A.K. Sangaiah, M. Shoaib, et al. An efficient computerized decision support system for the analysis and 3D visualization of brain tumor Multimed Tools Appl, 78 (2019), pp. 12723-12748 CrossRefView Record in ScopusGoogle Scholar

S. Iqbal, M.U. Ghani Khan, T. Saba, Z. Mehmood, N. Javaid, A. Rehman, et al. Deep learning model integrating features and novel classifiers fusion for brain tumor segmentation Microsc Res Tech, 82 (2019), pp. 1302-1315CrossRefView Record in ScopusGoogle Scholar

T. Saba, A.S. Mohamed, M. El-Affendi, J. Amin, M. Sharif Brain tumor detection using fusion of hand crafted and deep learning features Cogn Syst Res, 59 (2020), pp. 221-230 Article Download PDF View Record in Scopus Google Scholar

F. Ramzan, M.U.G. Khan, S. Iqbal, T. Saba, A. Rehman Volumetric segmentation of brain regions from MRI scans using 3D convolutional neural networks IEEE Access, 8 (2020), pp. 103697-103709 CrossRefView Record in ScopusGoogle Scholar

D.R. Nayak, R. Dash, B. Majhi Automated diagnosis of multi-class brain abnormalities using MRI images: a deep convolutional neural network based method Pattern Recognit Lett (2020) Google Scholar

Z. Lu, Y. Bai, Y. Chen, C. Su, S. Lu, T. Zhan, et al. The classification of gliomas based on a pyramid dilated convolution ResNet model Pattern Recognit Lett (2020) Google Scholar

A.A.A. Setio, F. Ciompi, G. Litjens, P. Gerke, C. Jacobs, S.J. Van Riel, et al. Pulmonary nodule detection in CT images: false positive reduction using multi-view convolutional networks IEEE Trans Med Imaging, 35 (2016), pp. 1160-1169 View Record in Scopus Google Scholar

W. Shen, M. Zhou, F. Yang, D. Yu, D. Dong, C. Yang, et al. Multi-crop convolutional neural networks for lung nodule malignancy suspiciousness classificationPattern Recognit, 61 (2017), pp. 663-673 Article Download PDF View Record in Scopus Google Scholar

H. Xie, D. Yang, N. Sun, Z. Chen, Y. Zhang Automated pulmonary nodule detection in CT images using deep convolutional neural networks Pattern Recogn, 85 (2019), pp. 109-119 Article Download PDF Cross Ref View Record in Scopus Google Scholar

H. Jiang, H. Ma, W. Qian, M. Gao, Y. Li, J. Hongyang, et al. An Automatic Detection System of Lung Nodule Based on Multigroup Patch-Based Deep Learning Network IEEE J Biomed Health Inform, 22 (2018), p. 1227 Cross Ref View Record in Scopus Google Scholar

S.M. Naqi, M. Sharif, A. Jaffar Lung nodule detection and classification based on geometric fit in parametric form and deep learning Neural Comput Appl (2018), pp. 1-19 View Record in Scopus Google Scholar

S.M. Naqi, M. Sharif, I.U. Lali A 3D nodule candidate detection method supported by hybrid features to reduce false positives in lung nodule detection Multimed Tools Appl, 78 (2019), pp. 26287-26311 Cross Ref View Record in Scopus Google Scholar

A. Asuntha, A. Srinivasan Deep learning for lung Cancer detection and classification Multimed Tools Appl (2020), pp. 1-32 Google Scholar

J. Premaladha, K. Ravichandran Novel approaches for diagnosing melanoma skin lesions through supervised and deep learning algorithms J Med Syst, 40 (2016), p. 96 Google Scholar

L.R. Bareiro Paniagua, D.N. Leguizamón Correa, D.P. Pinto-Roa, J.L. Vázquez Noguera, S. Toledo, A. Lizza Computerized medical diagnosis of melanocytic lesions based on the ABCD approach Clei Electron J, 19 (2016) 6-6 Google Scholar

S.A. Khan, M. Nazir, M.A. Khan, T. Saba, K. Javed, A. Rehman, et al.Lungs nodule detection framework from computed tomography images using support vector machine Microsc Res Tech (2019), 10.1002/jemt.23275 Google Scholar

N. Patel, A. Mishra Automated leukaemia detection using microscopic images Procedia Comput Sci, 58 (2015), pp. 635-642 ArticleDownload PDFView Record in ScopusGoogle Scholar

C. Zhang, S. Wu, Z. Lu, Y. Shen, J. Wang, P. Huang, et al. Hybrid Adversarial-Discriminative Network for Leukocyte Classification in Leukemia Med Phys (2020) Google Scholar

C.A. Hamm, C.J. Wang, L.J. Savic, M. Ferrante, I. Schobert, T. Schlachter, et al. Deep learning for liver tumor diagnosis part I: development of a convolutional neural network classifier for multi-phasic MRI Eur Radiol, 29 (2019), pp. 3338-3347 CrossRefView Record in Scopus Google Scholar

Y. Xu, L. Lin, H. Hu, D. Wang, W. Zhu, J. Wang, et al. Texture-specific bag of visual words model and spatial cone matching-based method for the retrieval of focal liver lesions using multiphase contrast-enhanced CT images Int J Comput Assisted Radiol Surg, 13 (1) (2018), pp. 151-164

F.P. Romero, A. Diler, G. Bisson-Gregoire, S. Turcotte, R. Lapointe, F. Vandenbroucke-Menu, et al. End-to-End discriminative deep network for liver lesion classification 2019 IEEE 16th International Symposium on Biomedical Imaging (ISBI 2019), IEEE (2019), pp. 1243-1246 Cross Ref View Record in Scopus Google Scholar

M.J. Jansen, H.J. Kuijf, W.B. Veldhuis, F.J. Wessels, M.A. Viergever, J.P. Pluim Automatic classification of focal liver lesions based on MRI and risk factors PLoS One (2019), p. 14 CrossRefGoogle Scholar

A. Ben-Cohen, H. Greenspan Liver lesion detection in CT using deep learning techniques. Handbook of medical image computing and computer assisted intervention Elsevier (2020) Google Scholar

M. Mharib, A. R. Ramli, S. Mashohor, and R. B. Mahmood, "Survey on liver ct image segmentation methods," The Artificial Intelligence Review, vol. 37, no. 2, p. 83, 2012.

S. Luo, X. Li, and J. Li, "Review on the methods of automatic liver segmentation from abdominal images," Journal of Computer and Communications, vol. 2, no. 02, p. 1, 2014.

N. Petrick, B. Sahiner, S. G. Armato, A. Bert, L. Correale, S. Delsanto, M. T. Freedman, D. Fryd, D. Gur, L. Hadjiiski et al., "Evaluation of computer-aided detection and diagnosis systems," Medical physics, vol. 40, no. 8, 2013

H. Hwang and R. A. Haddad, "Adaptive median filters: new algorithms and results," IEEE Transactions on image processing, vol. 4, no. 4, pp. 499–502, 1995.

Goshtasby and M. Satter, "An adaptive window mechanism for image smoothing," Computer Vision and Image Understanding, vol. 111, no. 2, pp. 155–169, 2008.

Pitas and A. N. Venetsanopoulos, "Order statistics in digital image processing," Proceedings of the IEEE, vol. 80, no. 12, pp. 1893–1921, 1992.

Rekeczky, T. Roska, and A. Ushida, "Cnn-based difference-controlled adaptive nonlinear image filters," International Journal of Circuit Theory and Applications, vol. 26, no. 4, pp. 375–423, 1998.

M. M. Rahman, M. S. Rana, M. A. Islam, M. M. Rahman, and M. H. Talukder, "A new filtering technique for denoising speckle noise from medical images based on adaptive and anisotropic diffusion filter," IJRCCT, vol. 2, no. 9, pp. 689–693, 2013.

M. Hilts and A. Jirasek, "Adaptive mean filtering for noise reduction in ct polymer gel dosimetry," Medical physics, vol. 35, no. 1, pp. 344–355, 2008.

S. Godsill, A. Doucet, and M. West, "Maximum a posteriori sequence estimation using monte carlo particle filters," Annals of the Institute of Statistical Mathematics, vol. 53, no. 1, p. 4, 2001.

N. S. Kota and G. U. Reddy, "Fusion based gaussian noise removal in the images using curvelets and wavelets with gaussian filter," Int. J. Image Process (IJIP), vol. 5, no. 4, pp. 456–468, 2011.

R. Adams and L. Bischof, "Seeded region growing," IEEE Transactions on pattern analysis and machine intelligence, vol. 16, no. 6, pp. 641–647, 1994.

Xu, D. L. Pham, and J. L. Prince, "Image segmentation using deformable models," Handbook of medical imaging, vol. 2, pp. 129–174, 2000.

Pham, C. Xu, and J. L. Prince, "Current methods in medical image segmentation," Annual review of biomedical engineering, vol. 2, no. 1, pp. 315– 337, 2000.

T. Leondes, Medical Imaging Systems Technology Volume 1: Analysis And Computational Methods. World Scientific Publishing Company, 2005, vol. 1.

Gadkari, "Image quality analysis using glcm," 2004.

M. M. Galloway, "Texture analysis using gray level run lengths," Computer graphics and image processing, vol. 4, no. 2, pp. 172–179, 1975.

B. Julesz, "Experiments in the visual perception of texture," Scientific American, vol. 232, no. 4, pp. 34–43, 1975.

S. R. Safavian and D. Landgrebe, "A survey of decision tree classifier methodology," IEEE transactions on systems, man, and cybernetics, vol. 21, no. 3, pp. 660–674, 1991.

K. Jain, J. Mao, and K. M. Mohiuddin, "Artificial neural networks: A tutorial," Computer, vol. 29, no. 3, pp. 31–44, 1996.

R. Pohle and K. D. Toennies, “Segmentation of medical images using adaptive region growing,” in Proc. SPIE Medical Imaging, vol. 4322, 2001, pp. 1337–1346.

D. Jimenez-Carretero, L. Fernandez-de Manuel, J. Pascau, J. M. Tellado, E. Ramon, M. Desco, A. Santos, and M. J. Ledesma-Carbayo, “Optimal multiresolution 3d level-set method for liver segmentation incorporating local curvature constraints,” in Engineering in medicine and biology society, EMBC, 2011 annual international conference of the IEEE. IEEE, 2011, pp. 3419–3422.

H. Foruzan, Y.-W. Chen, R. A. Zoroofi, A. Furukawa, Y. Sato, M. Hori, and N. Tomiyama, “Segmentation of liver in low-contrast images using k-means clustering and geodesic active contour algorithms,” IEICE TRANSACTIONS on Information and Systems, vol. 96, no. 4, pp. 798–807, 2013.

M. Erdt and M. Kirschner, “Fast automatic liver segmentation combining learned shape priors with observed shape deviation,” in Computer-Based Medical Systems (CBMS), 2010 IEEE 23rd International Symposium on. IEEE, 2010, pp. 249–254.

S. Luo, Q. Hu, X. He, J. Li, J. S. Jin, and M. Park, “Automatic liver parenchyma segmentation from abdominal ct images using support vector machines,” in Complex Medical Engineering, 2009. CME. ICME International Conference on. IEEE, 2009, pp. 1–5.